



3 1293 01025 0920

This is to certify that the

thesis entitled

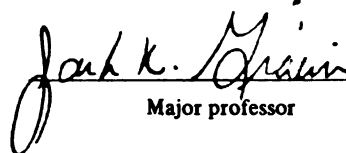
SORPTION OF ORGANIC PENETRANTS BY AMORPHOUS POLYAMIDE

presented by

MYUNGHOON LEE

has been accepted towards fulfillment
of the requirements for

MASTER degree in PACKAGING


Major professor

Date APRIL 1, 1994

LIBRARY
Michigan State
University

PLACE IN RETURN BOX to remove this checkout from your record.
TO AVOID FINES return on or before date due.

DATE DUE	DATE DUE	DATE DUE
APR 25 1995 FEB 0	_____	_____
MAR 05 1995	_____	_____
JUN 11 1997	_____	_____
FEB 02 1998 MAGIC 2	_____	_____
MAR 28 1999 JUN 17 1999	_____	_____
JUN 28 2000	_____	_____
AUG 28 2005 0531 06	_____	_____

MSU is An Affirmative Action/Equal Opportunity Institution

c:\circ\databus pm3-p.1

**SORPTION OF ORGANIC PENETRANTS BY AMORPHOUS
POLYAMIDE**

By

Myunghoon Lee

A THESIS

Submitted to

Michigan State University

in partial fulfillment of the requirements

for the degree of

MASTER OF SCIENCE

School of Packaging

1994

ABSTRACT

SORPTION OF ORGANIC PENETRANTS BY AMORPHOUS POLYAMIDE

By

Myunghoon Lee

Sorption studies involving the sorption of n-propanol by an amorphous nylon (Nylon 6I /6T) were carried out as a function of sorbate vapor activity at 23 °C.

Vapor activity levels from 0.035 to 0.91 were investigated to evaluate the concentration dependency of sorption mechanism.

Sorption behavior of propanol by Nylon 6I/6T showed distinctive two mode sorption phenomena as a function of vapor activity . At vapor activity levels below $a=0.11$, equilibrium sorption was achieved within a short period of time (less than 20 hours) , which can be interpreted as following a Fickian diffusion model.

A Langmuir- Flory-Huggins dual mode sorption model can also be applied at these concentration levels. However , for vapor activities above $a=0.11$, the sorption process appeared to be non-Fickian and resulted in a lack of equilibrium being attained.

ACKNOWLEDGEMENTS

I'd like to express my heartfelt thanks to my major advisor Dr. Jack . R . Giacin. His devoted and endless supports enabled me to complete this research. I would also like to thank Dr. Ruben Hernandez and Dr. Eric. A. Grulke for their precious advice and discussion throughout the course of research. I also thank to Dr. Heidi and Mr. Bob Hurwitz for helping me to design and assemble the test system and to provide comfortable circumstance during the research.

I am deeply indebted to the Korea Institute of Industrial Design and Packaging , which sent me to study in the School of Packaging. Finally , my lovely wife and two daughters deserve to have my deep thanks and love for their devoted supports during the research.

TABLE OF CONTENTS

	Page
LIST OF TABLES	v
LIST OF FIGURES	vi
INTRODUCTION	1
LITERATURE REVIEW	7
Characteristics of Amorphous Polymers	7
Properties of Amorphous Polyamide	9
Properties of Penetrant	13
Sorption Mechanisms	14
Ideal sorption and diffusion	14
Non ideal sorption	16
Modified dual mode sorption	20
Factors affecting the sorption process	22
Temperature	22
Crystallinity	25
Orientation	27
Sorption measurement	30

Diffusion and relaxation in glassy polymers	31
Correlation of sorption with penetrant size	33
MATERIALS AND METHODS	35
Polymer film	35
n-Propanol	35
Sorption measurement	36
Density experiment	39
RESULTS AND DISCUSSION	46
Data preparation and preliminary test	46
Equilibrium sorption	47
Analysis of sorption at vapor activity $a < 0.11$	49
Analysis of sorption at vapor activity $a > 0.11$	53
CONCLUSION	67
APPENDIX	
Appendix A Procedure for standard calibration curve constraction	68
Appendix B Electrobalance calibration procedure	70
Appendix C Vapor activity fluctuation	71
BIBLIOGRAPHY	76

LIST OF TABLES

Table	Title	Page
1.	Comparison of the properties between Amorphous Nylons and Nylon 66	12
2.	Relationship between rotameter readings and vapor activities	45
3.	Volume fraction vs. vapor activity from Flory-Huggins equation	51
4.	Average vapor activity and standard deviation in each step of vapor activity	52

LIST OF FIGURES

Figure	Title	Page
1.	Structure of Nylon 6I / 6T	10
2.	Structural formulas of various alcohols	13
3.	Schematic diagram of electrobalance test apparatus	41
4.	Saturated vapor pressure of n-propanol	42
5.	Standard calibration graph of n-propanol at 23 °C	43
6.	Illustration of sample flushing by nitrogen at 23 °C	44
7.	Evaluation of the reproducibility of the sorption system at $a = 0.06$	56
8.	Interval sorption of n-propanol at $a = 0 - 0.035$	56
9.	Interval sorption of n-propanol at $a = 0.035 - 0.050$	57
10.	Interval sorption of n-propanol at $a = 0.050 - 0.80$	57
11.	Interval sorption of n-propanol at $a = 0.080 - 0.110$	58
12.	Interval sorption of n-propanol at $a = 0.110 - 0.295$	58
13.	Interval sorption of n-propanol at $a = 0.295 - 0.390$	59
14.	Interval sorption of n-propanol at $a = 0.390 - 0.490$	59
15.	Interval sorption of n-propanol at $a = 0.490 - 0.840$	60
16.	Interval sorption of n-propanol at $a = 0.840 - 0.910$	60
17.	Successive interval sorption of n-propanol into Nylon 6I/6T at 23 °C ($a = 0 - 0.91$)	61

18.	Successive interval sorption of n- propanol into Nylon 6I/6T at 23 °C (a = 0 - 0.110)	61
19.	Experimental sorption isotherm for n-propanol in Nylon 6I/6T at the low vapor activities (a<0.11)	62
20.	Flory - Huggins plot when $\chi = 1.6$ from the equation $\ln a_1 = \ln V_1 + V_2 + \chi V_2^2$, $V_1 = 1 - V_2$	62
21.	Plot of M_t/M_∞ vs. $t^{1/2}$ for n-propanol sorption by Nylon 6I/6T, at 23 °C (a = 0 - 0.035)	63
22.	Plot of M_t/M_∞ vs. $t^{1/2}$ for n-propanol sorption by Nylon 6I/6T, at 23 °C (a = 0.035 - 0.050)	63
23.	Plot of M_t/M_∞ vs. $t^{1/2}$ for n-propanol sorption by Nylon 6I/6T, at 23 °C (a = 0.050 - 0.080)	64
24.	Plot of M_t/M_∞ vs. $t^{1/2}$ for n-propanol sorption by Nylon 6I/6T, at 23 °C (a = 0.080 - 0.110)	64
25.	Comparison between experimental and calculated data at vapor activity a =0.035	65
26.	Deviation from Equation(21) due to non - Fickian sorption for sorption of n-propanol by Nylon 6I/6T at 23 °C(a = 0.11 - 0.295): Graphic estimation of Fickian M_∞ value	65
27.	Plot of M_t/M_∞ vs. $t^{1/2}$ for n-propanol sorption by Nylon 6I/6T, at 23 °C; a = 0.11 - 0.295, Equation (21) for $M_\infty = 0.275$ and $t^{1/2} = 84$ sec.	66
28.	Plot of M_t/M_∞ vs. $t^{1/2}$ for n-propanol sorption by Nylon 6I/6T, at 23 °C; a = 0.11 - 0.295 ; points observed curve,Equation(21) for $M_\infty = 0.275$ and $t^{1/2} = 84$ sec.	66

29.	Distribution of vapor activity at $a = 0.035$	71
30.	Distribution of vapor activity at $a = 0.050$	71
31.	Distribution of vapor activity at $a = 0.080$	72
32.	Distribution of vapor activity at $a = 0.110$	72
33.	Distribution of vapor activity at $a = 0.295$	73
34.	Distribution of vapor activity at $a = 0.390$	73
35.	Distribution of vapor activity at $a = 0.490$	74
36.	Distribution of vapor activity at $a = 0.840$	74
37.	Distribution of vapor activity at $a = 0.910$	75

INTRODUCTION

Over the past decade , the development and use of high barrier plastic materials has increasingly replaced traditional glass and metal containers for food and beverage packaging.

The advantages of plastic packaging are numerous and include : low cost , light weight , a wide range of mechanical properties ,transparency, flexibility , direct food contact , and general consumer preference because of convenience and microwaveability (Salame , 1986).

However , with the use of plastic packaging there are concomitant concerns related to product / package interactions. This is a broad based topic that includes transport of gases and organic vapor of low molecular weight : (i) from the product through the package , as well as (ii) from the environment through the package to the product.

The specific mass transport (permeability) process may be described as a function of penetrant concentration , temperature , and time to equilibrium, as well as the composition of the penetrant / polymer system.

Therefore , polymer structure , free volume , chain stiffness or segmental mobility , and the availability of specific sites of interaction in the polymer,plus the physicochemical characteristics of the penetrant (gas, water vapor , or organic vapor) determine the mode and mechanism of sorption

and thus , the resultant transport and mechanical properties of the polymer (Blatz , 1989).

The dual mode sorption model has been widely used to describe the solubility of gases in glassy polymers , and in glassy , polar polymers as well. This model assumes that the solute molecules in the glassy polymer consist of non-specifically absorbed and specifically adsorbed species , which are in dynamic equilibrium in the medium (Michaels et al., 1963)

The solubility of the absorbed species is represented by Henry's law , and the solubility of the adsorbed species is described by a Langmuir type adsorption isotherm. The Langmuir sorption is believed to occur at specific sites , usually considered to be units of stable free volume present in the amorphous polymer structure.

Local equilibrium between the absorbed and adsorbed populations is maintained throughout the polymer matrix. The total amount of solute sorbed by both mechanisms is :

$$C = C_D + C_H = K_D P + \frac{C_H' b}{1 + b p} \quad (1)$$

where C is the total concentration of sorbed solute in the polymer , C_D and C_H are the solubilities due to absorption (Henry's Law) and Langmuir type adsorption respectively , K_D is the Henry's law

constant , b is the hole affinity constant , C_H' is the hole saturation constant and p is the pressure.

Recently , Hernandez et al. (1991) have studied the sorption of water vapor into an amorphous polyamide (Nylon 6I / 6T). The authors have applied a dual mode sorption model , based on Langmuir and Flory - Huggins equations , to describe the sorption process. The total amount of water sorbed by the polymer was described by the summation of a Langmuir type association , and by a solution component mode given by the Flory-Huggins model , which is given by:

$$V_1 = V_1^L + V_1^{FH} \quad (2)$$

Where V_1 is the total volume fraction of water within the polymer , and the superscript L and FH refer to Langmuir and Flory - Huggins water sorption contributions , respectively. These contributions are expressed as :

$$V_1^L = \frac{K a}{1 + B a} \quad (3)$$

and

$$a = \exp [\ln V_1^{FH} + (1 - V_1^{FH}) + \chi (1 - V_1^{FH})^2] \quad (4)$$

Where a is water activity , χ is the Flory - Huggins interaction parameter , and K and B are parameters of the Langmuir equation (Hernandez et al., 1991).

The behavior of oxygen solubility within the polymer / water system

was related to V_1L , according to the following expression.

$$V_{O_2} = V^* - F V_1L \quad (5)$$

where V_{O_2} is the solubility of oxygen in the polymer as a function of a , V^* is the solubility of oxygen in the dry polymer, and F is a factor that relates sorption values of oxygen at dry conditions and the fraction volume of water described by the Langmuir sorption mode, when water activity equals one. The fact that 80 % of the total oxygen dissolved by the polymer at dry conditions was displaced by molecules of water associated with active sites of the polymer matrix, indicated the importance of these active sites in the mechanism of the solubility of oxygen within the Nylon 6I / 6T bulk phase. These results also suggested that molecular size may be an important factor in determining the final equilibrium sorption values in the three component system of polymer, water and oxygen (Hernandez et al., 1991).

Based on the results described above, it can be proposed that a similar model can be applied to the binary system of polymer and organic penetrants, which has not yet been reported.

A quantitative relationship between molecular weight of sorbates and active sites concentration in polyethylene was reported by Gedraitite et al. (1989), who studied the sorption by polyethylene, of selected low molecular weight compounds dissolved in *n*-hexane, and in isopropanol.

In addition to the limited amount of data describing the effect of moisture content on the mass transport and solubility of oxygen in hydrophilic polymers, no references have been found in the literature which considered the importance of size distribution of sorption sites in determining the final equilibrium sorption values for the sorption of organic penetrants by hydrophilic polymers, such as the amorphous polyamide.

There is also a paucity of data describing the effect of organic vapor concentration on the solubility and diffusion of organic penetrants in hydrophilic polymers, and the importance of active binding sites associated with the polymer matrix in determining the final equilibrium sorption value for the binary system of polymer / organic vapor.

The proposed studies will provide for a better understanding of the parameters contributing to the diffusion and sorption of organic penetrants in hydrophilic polymer membranes.

In terms of practical application, the data obtained describing the relationship between sorption parameters and the molecular weight of the sorbate molecule may allow calculation of the solubility of a penetrant in the polymer matrix from knowledge of the penetrants solubility in a contact phase, and its molecular weight. This could further provide a means of designing a barrier structure for a specific end use application.

For example, in the packaging of a juice product, when there is concern for flavor loss due to sorption, or sorption of ingredients from a

pharmaceutical preparation , which could result in loss of product efficacy.

Objectives

1. Determine the equilibrium sorption isotherm for n-propanol in an amorphous polyamide (Nylon 6I / 6T) at water activity = 0.
2. Provide an empirical framework to study the sorption of organic vapor by a glassy polymer , and the relationship of Langmuir type association (active site binding) , to the solubility of organic penetrants in hydrophilic polymers.
3. Evaluate the appropriateness of the Langmuir-Flory-Huggins dual mode sorption model to describe the sorption isotherm of n-propanol in the amorphous polyamide (Nylon 6I / 6T).

LITERATURE REVIEW

Characteristics of Amorphous Polymers

A vast majority of well-known polymers are characterized by their structural differences. The conformation of flexible chain molecules in the melt or glassy state is determined both by the local position and orientational distribution of chain segments belonging to the same chain (intramolecular correlations) or belonging to different chains (intermolecular correlations) (Wendorff , 1987).

Polymers differ from other low molecular weight organic or inorganic materials , in that they are composed of long chain molecules , usually containing a huge number of atoms. This gives rise to a very large number of internal degrees of freedom for flexible chain molecules (Blumstein , 1978). The chain is represented by a line in space , the curvature of which depends upon the persistence length A_i . The parameter(A_i) is thus a measure of the chain stiffness. It corresponds to the distance along the chain over which correlations in the orientation of successive chain units extend. The mean square end-to-end distance $\langle h^2 \rangle$ is given by

$$\langle h^2 \rangle / 2 A_i L = [1 - (1 / x)] [1 - \exp (-x)] \quad (6)$$

where L is the contour length of the chain and $x = L / A_i$. A worm- like chain becomes a flexible Gaussian chain for $x \rightarrow \infty$, and a rigid rod- like

chain for $x \rightarrow 0$ (Wendorff , 1987).

Flexible chain molecules have a persistence length of the order of 1 or 2 nm. A flexible chain in a random configuration occupies only a small portion of the space it pervades. The density of an isolated chain molecule is typically of the order of 1 % of that of the condensed state , and it decreases with increasing chain length (Wendorff , 1987).

Intermolecular forces require , however , that the empty space be filled in the condensed , amorphous state. This may be achieved in various ways as described below.

- (1) The chains may collapse , a process which is known to occur in solutions with poor solvents (Williams et al. , 1981) ;
- (2) The chains may aggregate in bundles in which neighboring chains or chain segments are parallel to each other as in a nematic liquid crystalline phase (Pechhold et al. , 1979) ;
- (3) The chains may remain in their random configuration and many different chains are able to pervade the space taken up by the reference chain.

This leads to a highly entangled system (Gennes , 1979).

The distribution of the centers of the chains as well as their orientation is as close to random , as in a real gas. Macroscopic properties of amorphous polymers are known to depend heavily on the local spatial and orientational distribution of chain segments , belonging to the same or to a different chain (Wendorff, 1987).

Properties of Amorphous Polyamide

Polyamides containing aromatic residues are normally very high melting, highly insoluble semi-crystalline materials , which are difficult to process.

In recent years , a number of more easily processed amorphous polyamides , based on iso- and terephthalic acids have been claimed in the patent literature. In general , amorphous polyamides can possess a wide range of good mechanical properties , including tensile and impact strength , and a high specific modulus , which are desirable for engineering applications (Dolden , 1976).

The amorphous polyamide (Nylon 6I / 6T) which was developed by the E.I.Du pont De Nemours & Co., Ltd., has a random structure based on hexamethylenediamine and a 70 / 30 mixture of isophthalic and terephthalic acids (Fig. 1), and when dry has a glass transition temperature (T_g) of 125 ° C (Blatz , 1989).

It has good processability by primary extrusion and molding operations , as well as secondary processing such as thermoforming. Film has been produced by both the blown film and flat cast processes. Coextruded film and sheet can be produced using three to five layers , at thicknesses from 2 mils to 60 mils.

$\text{NH}_2\text{CH}_2 - (\text{CH}_2)_4 - \text{CH}_2\text{NH}_2 \rightarrow \text{Hexamethylene diamine}$

+

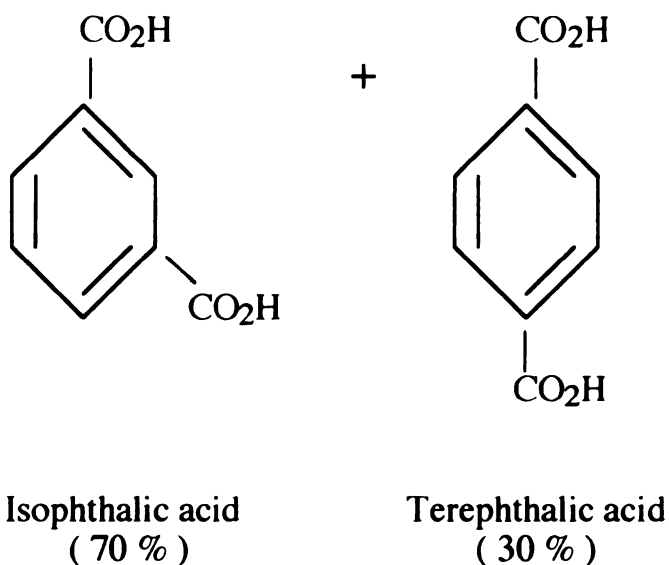


Figure 1. Structure of the Nylon 6I / 6T

Nylon 6I / 6T also has good tensile strength , elongation and tensile modulus. These properties are similar to those for the other resins used for quality packaging applications. The tensile strength of amorphous polyamide is higher than nylon 66 dry , but decreases in a manner similar to nylon 66 at 50 % RH. The tensile modulus , a measure of stiffness , shows an atypical trend with increasing humidity. As expected , the modulus of nylon 66 decreases substantially as the humidity increases , however the modulus of amorphous polyamide

increases slightly. Thus, it maintains its stiffness at high humidities (Blatz, 1989).

The barrier properties of amorphous polyamide approaches the levels of polyvinylidene chloride, ethylene vinyl alcohol copolymer and the extrudable acrylonitrile copolymers. As was previously indicated, water vapor has an unexpected effect on the permeability of amorphous polyamide. Whereas the oxygen permeability of nylon 66 film increases on exposure to water vapor, that for the amorphous polyamide film decreases. Thus, a film of amorphous polyamide has a significantly better barrier as the humidity increases (Blatz, 1989).

The chemical resistance is usually not as good as the semi-crystalline resins, such as PET or 6 and 66 Nylon. The resin is unaffected by dilute acids and bases, but is attacked by acetic acid (Blatz, 1989).

It is also attacked by the common low molecular weight alcohols such as ethyl alcohol and solutions containing more than 10 % ethyl alcohol.

The amorphous nylon is resistant to both aliphatic and aromatic hydrocarbons, to chlorinated solvents, ketones, and esters. However, methylene chloride will cause swelling (Blatz, 1989).

As with all glassy polymers, as the melt is cooled down and reaches the glass transition temperature (T_g), the molecular motions are frozen at that temperature, which results in a void content that is higher

than that in a polymer with low T_g . For an amorphous glassy polymer . the larger the difference in temperature between the T_g and the test temperature the greater the amount of unrelaxed volume (sometimes called the free volume). Table 1 summarizes selected mechanical and barrier properties of amorphous nylon (Nylon 6I / 6T) and nylon 66.

Items	Unit	Amorphous Nylon*	Nylon 66
Tensile strength	K Psi	10.0	8.0
Elongation	%	50.0	70.0
Tensile modulus	K Psi	330	340
Heat deflection T.	@ 66 psi	261 ° F (128 ° C)	365 ° F (185 ° C)
of packaging resin	@ 264 psi	248 ° F (120 ° C)	151 ° F (66 ° C)
Oxygen	Dry	3.3	2.5
Permeability (1)	50 % RH	1.4	5.0
CO ₂		8.0	10.0(50 % RH)
Permeability (2)			
Water vapor		5.0	5.7
Permeability (3)			

* SELAR® PA of Du Pont Co.,

(1) CC-mil / 100 SQ. IN. / 24 Hours-Atm. at 30 ° C

(2) CC-mil / 100 SQ. IN. / 24 Hours- Atm. at 80 % RH, 30 ° C

(3) g-mil / 100 SQ. IN. / 24 Hours- Atm. at 90 % RH, 23 ° C

Table 1. Comparison of mechanical and barrier properties of amorphous nylon* and nylon 66

Properties of penetrant : 1 - Propanol

Alcohols may be viewed as alkyl derivatives of water and are indicated by the formula R - OH. They are structurally similar to water , but have one of the hydrogens replaced by an alkyl group.

The reactions of alcohols are those of the -OH functional group , known as the hydroxyl group .

Figure 2 lists both the IUPAC and common names for a variety of simple alcohols , which include the 1 - propanol used in this study.

CH_3OH	$\text{CH}_3\text{CH}_2\text{OH}$	$\text{CH}_3\text{CH}_2\text{CH}_2\text{OH}$
methanol methyl alcohol	ethanol ethyl alcohol	1-propanol n-propyl alcohol
$\begin{array}{c} \text{CH}_3\text{CHCH}_3 \\ \\ \text{OH} \end{array}$	$\begin{array}{c} \text{CH}_3\text{CHCH}_2\text{OH} \\ \\ \text{CH}_3 \end{array}$	$\begin{array}{c} \text{CH}_3 \\ \\ \text{CH}_3\text{COH} \\ \\ \text{CH}_3 \end{array}$
2-propanol isopropyl alcohol	2-methyl-1-propanol isobutyl alcohol	2-methyl-2-propanol tert-butyl alcohol

Figure 2. Structural formulas of alcohols.

Sorption Mechanisms

Organic vapors can exhibit concentration dependent mass transport and sorption processes. The permeant vapor pressure and the type of vapors that come in contact with the package will also determine the magnitude of sorption and permeation into and out of polymeric packaging systems.

The study of the solubility of gases in polymers has a twofold objective : (1) it permits the establishment of correlations of gas solubilities , with readily available gas molecular parameters ; and (2) it also supplies information on the morphology of polymers (Vieth ,1966).

Ideal sorption and diffusion

In ideal gas - polymer systems , both the solubility and diffusion coefficients are constant at any given temperature , and so the permeability is also a constant.

Permeation or transport through a polymer film can be described in terms of its component parts by Equation (7):

$$P = D S \quad (7)$$

where S is the solubility coefficient , and D is the diffusion coefficient.

S characterizes the amount of permeant that can be dissolved into the

polymer under the given vapor pressure , and D describes the rate at which the permeant molecules are advancing through the barrier film.

For a simple permeation process , the sorption and desorption steps are described by the assumption of Henry's law , which relates the concentration of the penetrant in the polymer , to the vapor pressure in equilibrium with the polymer. The partial pressure of the penetrant is further related to the penetrant concentration in the gas phase through the ideal gas law.

Generally , the application of the ideal gas law is justified since the concentration of the diffusant in the gas phase is very low. The diffusion step is described by Fick's first (8) and second laws (9) of diffusion (Hopfenberg , 1973).

$$F = - D(c) \frac{\partial c}{\partial x} \quad (8)$$

$$\frac{dc}{dt} = \frac{\partial}{\partial x} \left(D(c) \frac{\partial c}{\partial x} \right) \quad (9)$$

where F is the flux or the rate of transfer of penetrant per unit area , expressed as mass of diffusant per unit area per time ; c is the concentration of the penetrant in the film , expressed in the same unit of mass of diffusant per unit of volume or mass of the polymer.

D is the mutual diffusion coefficient , in (length)²/ time ; t is time ; and x is the length in the direction in which transport of the penetrant

molecules occurs.

To obtain the flux (F) or the diffusion coefficient (D) from Equations (8) or (9), initial and boundary conditions associated with the experimental method are needed, and the expressions solved to give the desired values.

It should be recognized that when the diffusion coefficient is calculated using Equations (8) and (9), only approximate values will be obtained.

More accurate estimations of this parameter can be carried out by using, for example, a nonlinear maximum likelihood sequential method, based on the Gauss linearization method (Beck and Arnold, 1977).

The partial pressure of the penetrant is further related to the penetrant concentration in the gas phase through the ideal gas law. Application of the ideal gas law is justified since the concentration of the diffusant in the gas phase is, in general, very low (Hernandez et al., 1986).

Non-ideal sorption

The sorption of a low molecular weight compound proceeds by two steps. Firstly the sorbate penetrates into the relatively ordered polymeric substance, forming a true solution. The concentration of the homogeneously dissolved compound is related to the concentrations outside the polymer by Henry's Law. Secondly the dissolved compound is

reversibly sorbed by certain centers , which are the zones of destruction of the short range order. The total sorbate concentration in the polymer will be the sum of the concentrations of the homogeneously dissolved compound, and of that sorbed by the sorption centers (Shlyapnikov and Mar'in , 1987).

For systems in which the solubility doesn't conform to Henry's law , both the diffusion and the solubility parameters are concentration dependent. The solubility coefficient often is essentially constant at low vapor activities for the more volatile vapors, and only the diffusion coefficient exhibits significant concentration dependence (Rogers et al. , 1960). This concentration dependence can be understood in the context of the free volume theory (Cohen and Turnbull , 1959 ; Fujita , 1961; Kwei and Wang, 1972 ; Peterlin , 1975) , which gives a relationship between the diffusion coefficient D and the fractional free volume f :

$$D = A \exp (- B / f) \quad (10)$$

where A is a frequency factor and B is a measure of the minimum hole size for the jump process (Choy et al. , 1984). Fujita (1961) further assumed that

$$f = f_0 + \beta C_s \quad (11)$$

where C_s is the mass fraction of the penetrant and β denotes the effectiveness of the penetrant molecule for increasing the free volume of the polymer. Substituting Equation (11) into Equation (10) and assuming $\beta C_s \ll f_0$, Equation (10) becomes

$$D = D_0 \exp (\gamma C_s) \quad (12)$$

where

$$\gamma = B\beta / f_0^2 \quad (13)$$

Peterlin (1975) has obtained an alternative expression for γ in terms of the fractional free volume of the penetrant , but the physical meaning is essentially the same.

Equation (13) shows that the concentration coefficient γ depends on f_0 and β ; i.e., γ is a function not only of the fractional free volume but also of the interaction between the penetrant and the polymer. For the two penetrant-polymer systems , methylene chloride-HDPE and methylene chloride-LDPE , β does not seem to vary significantly with drawing , so the change in γ is determined largely by the $1 / f_0^2$ factor , which gives rise to a substantial increase in γ with increasing draw ratio (Choy et al. , 1984).

The idea that the molecules of the penetrant present in a polymer are of two different types (those mobile , homogeneously dissolved , and those immobile , sorbed in certain centers) , was called the dual mode sorption model. This model has been widely applied to describe nonideal sorption , which can explain the irregularities of diffusion and sorption of low molecular weight compounds (i.e. , additives) in glassy polymers (Paul and Koros , 1976).

The magnitude of the negative enthalpies of sorption reported by

Mears (1954) for neon , nitrogen , oxygen and argon in glassy polyvinyl acetate and by Barrer et al. (1957) for organic vapors in ethyl cellulose were inconsistent with the sorption theories of rubbery systems , and led Barrer et al. to suggest a two-mode , concurrent sorption mechanism for glassy polymers , namely ordinary dissolution and 'hole' filling. In glassy polymers , substantial deviations from linearity are often observed in sorption isotherms at penetrant pressures above 1 atm.

Barrer et al. (1957) first suggested that two distinct mechanisms may be operating in the sorption of low molecular mass species by glassy polymers. They observed isotherms for the sorption of C₄ and C₅ isomers in glassy ethyl cellulose that curved towards the pressure axis , and appeared to become asymptotically linear at high penetrant pressures.

These results were interpreted in terms of a "dual mode" sorption model , which assumes a combination of Langmuir - type trapping within preexisting vacancies , plus "true" Henry's law solution. Quantitatively , this may be written :

$$C = K_D p + \frac{C'_H p}{1 + b p} \quad (14)$$

where C is the total sorbate concentration , K_D is the effective Henry's law solubility constant , C'_H is the Langmuir "capacity factor", b is the Langmuir site affinity parameter , and p is the gas pressure.

Michaels et al. (1963) also reported the sorption of helium , nitrogen , oxygen , argon and methane in glassy amorphous , and glassy semi-crystalline polyethylene terephthalate. For penetrant partial pressures up to 1.0 Henry's law was followed. However , carbon dioxide at 25 ° C and 40 ° C , and ethane at 25 ° C, in the same pressure range , deviated from Henry's law.

The carbon dioxide isotherms prompted Michaels et al. (1963) to propose a two - mode sorption model of ordinary dissolution and adsorption in microvoids ('holes') , for gas sorption in glassy amorphous polymers.

Michaels and Bixler (1961) attempted to adapt the Flory - Huggins theory of polymer solution to the sorption of simple gases, picturing the process as first condensation of the gas , followed by mixing of the polymer and liquid penetrant.

Modified dual mode sorption model

Recently , Hernandez et al. (1991) also proposed a modified dual mode sorption model , which described the sorption of water vapor by an amorphous polyamide at 23 ° C. They modified Eqn. (14) by using the Flory-Huggins equation to describe non-specific solution , rather than Henry's Law. This modification allowed the model to fit over the

activity range , $0 < a < 1$. Although other choices for the solution model are possible , they applied the Flory - Huggins Equation (15) because of its simplicity.

$$\ln a = \ln V_1 + V_2 + \chi V_2^2 \quad (15)$$

where χ is the interaction parameter. The non-specific sorption term is nonlinear , the complete model can have an inflection point and should predict clustering somewhere over the range of activity values (Hernandez et al., 1990). The modified dual mode sorption model is expressed in terms of volume fractions and solute activity:

$$V_1 = V_1^{FH} + V_1^L \quad (2)$$

where V_1^{FH} refers to the Flory - Huggins contribution to the solute volume fraction , and V_1^L is Langmuir volume fraction contribution.

Since Equation (2) is nonlinear , it is convenient to determine the value for V_1^{FH} by numerical methods , such as Newton - Raphson technique and Equation (2) becomes:

$$V_1 = FH (a , \chi) + \frac{K a}{1 + B a} \quad (16)$$

Factors affecting sorption behavior

Temperature

The temperature dependence of the sorption parameters have been studied for a number of penetrant / polymer systems. The K_D and b terms are generally decreasing as a function of T , and appear to be well correlated at a given temperature with the penetrant Lennard - Jones energy parameter ϵ/κ values (Pace and Datyner , 1980-). The data for C'_H are more ambiguous.

Some results suggest that C'_H is independent , or varies only weakly with temperature , and others suggest that C'_H is a strongly decreasing function of T (Pace, 1980). However, it is reasonable to assume that the immobile species is contained in microvoids formed by local segmental motions in the rubbery state which have become "frozen" in the glass.

This frozen void fraction must be , to a first approximation , at least independent of T to explain the low thermal expansivity of the glass , which is comparable to that of the crystalline state. Hence C'_H should also be essentially independent of T (Pace and Datyner , 1980).

The glass transition temperature (T_g) of any amorphous substance , whether polymeric or not , is defined as the point where the thermal expansion coefficient undergoes a discontinuity. In polymers , there

expansion coefficient undergoes a discontinuity. In polymers, there may be more than one discontinuity associated with the thermal expansion coefficient term.

The largest discontinuity is usually associated with the loss of the molecular mobility, which permits configurational rearrangements of the chain backbones (Ferry, 1970).

Below the T_g of a polymer, not enough energy is provided to produce the Micro-Brownian motion of chain segments 20-50 carbon atoms in length, and the chains are locked into the position created from the processing history. Sorption and diffusion in polymers at temperatures below the polymer's T_g consist of more complex behaviors, and are not well understood at this time (Hernandez, 1984).

Above the T_g of a polymer, it seems likely that hole filling is an important sorption mechanism, which is supported by the fact that the low-pressure (Henry's law) solubility for simple gases varies smoothly on going through T_g , although the apparent heats of solution are different and constant in the glassy and rubbery regions.

Meares (1957) proposed the following idealised concept of the gaseous sorption and diffusion process in polymers at temperatures above and below T_g , based on the relative activation energies for diffusion and heats of solution for polyvinyl acetate in the two temperature regimes, and the zone

of activation theory.

Above T_g , gas molecules which dissolve in the polymer must create their own "holes" by separating the interchain polymer contacts.

The penetrant then diffuses through the polymer matrix along cylindrical voids created by the synchronized rotation of polymer segments about the C - C bonds (Meares , 1957). Below T_g , the polymer consists of regions of densely packed and arranged chains which have limited freedom for rotation, separated by less dense regions of disordered chains that form the 'holes' into which the gas sorbs. The gas molecules diffuse between these 'holes' by the slight compressing of localized chains in the dense regions enabling the gas molecules to pass through. This compression in the glassy state does not create the long cavities common to the rubbery state, indicating that the zone of chain activation is much larger in the rubbery state. This zone of activation was found to be essentially independent of the size of the penetrating molecule (Meares , 1954).

Above the T_g the polymer is assumed to be in thermodynamic equilibrium, while below T_g the hole concentration is that which was frozen in at T_g , provided the glass is formed by slow cooling from the rubbery region. One therefore expects

$$C'_H = C_o \exp (- H_h / RT) , \quad T > T_g \quad (17 a)$$

$$C'_H = C_o \exp (- H_h / RT_g) , \quad T < T_g \quad (17 b)$$

where H_h is the enthalpy of hole formation , C_o is a pre-exponential term , and R is the gas constant ; b is also expected , over moderate temperature ranges , to have a van't Hoff form

$$b = b_o \exp (- E_{ad} / RT) \quad (18)$$

where E_{ad} is the energy change of hole filling. Either above or below T_g , gas sorption may be thought to take place either :(1) within an existing hole , or (2) at a "site" on the polymer lattice , after creating a hole at that point (Pace and Datyner , 1980).

Crystallinity

It is assumed that even the smallest gas molecule cannot penetrate or diffuse through a polymer crystallite. Therefore , the higher the degree of crystallinity in a polymer , the lower the permeability.

Michaels et al.(1961) have found that the solubility constants for a particular gas were proportional to the amorphous volume fraction , α , that is :

$$K = \alpha K^* \quad (19)$$

where K^* is the solubility constant of a hypothetical completely amorphous polyethylene , and K is the solubility constant of partially crystalline polyethylene. This relationship suggests that the gases are sorbed entirely

in the amorphous phase of rubbery crystalline polymers , and that the quantity sorbed is directly proportional to α (Hopfenberg and Stannet , 1973).

The relationship discussed in Equation (19) was used by Michaels et al. (1963) in studying the effect of crystallinity on the sorption of several gases in glassy semi-crystalline polyethylene terephthalate.

Unlike the rubbery semi-crystalline polyethylene , it was found that gas solubility , with the exception of helium , is not directly proportional to the amorphous volume fraction. The decrease in solubility accompanying crystallization , $(C^* - C) / C^*$ (C^* is the amorphous polymer solubility and C is the crystalline polymer solubility), was smaller than the corresponding reduction in amorphous volume fraction , $1 - \alpha$; and this solubility decrease on crystallization tended to become less with increasing Lennard - Jones force constants , ϵ / κ of the sorbed gas.

This result can be satisfactorily accounted for in terms of the 'hole' model of the glassy amorphous phase. Upon annealing the polymer ,it is more probable that the denser regions crystallize first , tending to remove more of the amorphous phase used for gas dissolution , therefore leaving the residual amorphous phase with a higher concentration of 'holes' than in the previously amorphous polymer. This means that crystallization in glassy polymers tends to increase the relative contribution of 'hole' filling as indicated by the C'_H / a values ; by definition the 'hole' saturation - limit per

unit volume amorphous phase. Also such an increase in concentration of 'holes' with increasing crystallization accounts for the decreased reductions in solubility with increasing ϵ / κ of the gas, a measure of the tendency of the gas to condense (Michaels et al., 1963).

Michaels et al.(1963) generalized their original dual sorption model to include the effects of crystallinity on the solubility of the dissolved species as shown in Equation (20).

$$C = \frac{C_H b p}{1 + b p} + \alpha K^* D p \quad (20)$$

The usual methods for assessment of degree of crystallinity in nylons are by measurement of density, differential scanning calorimetry (DSC) or by infrared techniques. Density measurement is perhaps most satisfactory because it is rapid, precise, and unaffected by sample calibration - the assumption of amorphous and crystalline densities.

Orientation

Polymer chain orientation will "line - up" the crystallites, and cause the permeating molecule to take a more tortuous path.

Vieth et al. (1961) have investigated the effects of chain orientation. The sorption mechanism was found to be similar in oriented and unoriented

polyethylene terephthalate , but the solubility of gas is higher in the oriented film. An analysis of the sorption data gives higher Henry's law solubility constants , higher hole-filling constants , and higher hole affinity constants in the oriented polyethylene terephthalate film. The diffusion of vapors into a two dimensionally restricted piece of polymer will result in the polymer molecules being oriented and extended in the direction of diffusion (Hartley, 1946). A number of ingenious optical experiments were devised to illustrate these effects. Hartley (1946) also studied directly the effect of orientation on the rate of penetration of solvents by stretching cellulose acetate films and following the sorption optically.

The oriented samples were penetrated up to 24 times faster than the unoriented films. Hartley suggested that the higher sorption rate was due at least partly to the greater transverse oscillation of the polymer chains contributing to the sorption process. The magnitude of the penetrant activity not only affects the rate of sorption but the relative contributions of Fickian diffusion and relaxation controlled transport.

The penetrant activity , therefore, biases the effect of orientation on these processes. At low activities Fickian diffusion predominates , and the effect of orientation on the Fickian diffusion rate is small.

Conversely , at high activities where the transport is controlled by polymeric relaxations , the relaxation rate is a strong function of orientation , which in turn strongly affects the rate of sorption.

Choy et al. (1984) studied the sorption and diffusion of toluene vapor at 30 ° C in polypropylene with draw (orientation) ratio from 1 to 18.

Drawing leads to the transformation of the initially spherulitic material into the fibrous structure , with many taut tie molecules lying mainly on the outer boundary of the microfibrils. The free volume and hence the sorption sites are thereby reduced , and the microfibrils become less and less permeable as the draw ratio increases. As a result , the equilibrium concentration and the zero concentration diffusion coefficient drop by factors of 4 and 30 , respectively. The diffusion coefficient increases exponentially with toluene concentration but the concentration dependence becomes weaker with increasing draw ratio , indicating that the severely constrained chain segments in the drawn samples have much less freedom to mix with penetrant molecules (Choy et al. , 1984).

Sorption measurement

Sorption experiments are usually carried out at equilibrium vapor pressure , using a gravimetric technique in an apparatus that records continually the gain or loss of weight by a test specimen as a function of time (Hernandez et al. , 1986).

The diffusion equation appropriate for the sorption of penetrant by a polymer sample in sheet or film form was described by Crank (1975) as :

$$\frac{M_t}{M_\alpha} = 1 - \frac{8}{\pi^2} \left[\exp\left(-\frac{D \cdot \pi^2 \cdot t}{L^2}\right) + \frac{1}{9} \exp\left(-\frac{9 D \cdot \pi^2 \cdot t}{L^2}\right) \right] \quad (21)$$

where M_t and M_α are the amount of penetrant sorbed by the polymer film sample at time (t) and the equilibrium sorption level after infinite time , respectively ; t is the time to attain M_t , and L is the thickness of the film sample.

The sorption diffusion coefficient (D_s) can be calculated from Equation (21) by setting M_t / M_α equal to 0.5 and solving to give D_s .

$$D_s = \frac{0.049 L^2}{t_{0.5}} \quad (22)$$

where $t_{0.5}$ is the "half-sorption time" or the time required to attain the value ,
 $M_t / M_\alpha = 0.5$

Diffusion and relaxation in glassy polymer

It is now widely agreed that transport involves both a diffusion process , controlled by a concentration gradient , and a relaxation process , controlled by a time dependent response of the polymer to a swelling stress. The observed effects may vary not only with the particular polymer / penetrant system considered , but also with the range of vapor activities or concentrations covered in specific experiments (Berens , 1977). Logers (1965) has pointed out that sorption vs. time curves may be pseudo-Fickian , sigmoid , or two stage as the penetrant concentration is increased. Hopfenberg (1970) has also pointed out , however , that at the low temperatures and activities , where simple Fickian behavior in the glassy state might be expected , experimental times become prohibitively long with conventional polymer film samples. Berens and Hopfenberg (1977) reported that sorption by initially penetrant free polymer samples is dominated by a rapid Fickian diffusion process , while incremental sorptions show larger relative contributions from slow relaxation processes. The relaxation processes appear to be related to slow redistribution of available free volume through relatively large scale segmental motions in the relaxing polymer. The diffusion - relaxation model seems to provide a meaningful analysis of several non - Fickian "anomalies" , including a very slow

approach to apparent equilibrium , two stage and sigmoidal sorption curves , and sorption curves involving an initial maximum followed by temporary desorption and subsequent resorption (Berens and Hopfenberg , 1977).

In sorption experiments at very low activities , simple Fickian kinetics were obeyed and equilibrium was achieved within a short time. In sorption experiments covering a larger concentration interval , the initial rapid sorption was followed by a slower further uptake of penetrant which was qualitatively attributed to a relaxation - controlled swelling process (Berens and Hopfenberg , 1977).

Berens (1977) suggested the sorption model for the vinyl chloride monomer by polyvinyl chloride powder sample , which can be useful for calculation of numerical values of equilibrium and kinetic parameters ; the equation is

$$M_t = M_{\infty,F} \left[1 - \frac{6}{\pi^2} \sum_{n=1}^{\infty} \frac{1}{n^2} \exp(-n^2 k_F t) \right] + \sum_i M_{\infty,i} [1 - \exp(-k_i t)] \quad (23)$$

where $M_{t,F}$ is the contributions of the Fickian process at time t , k_i is the respective relaxation rate constant and each $M_{\infty,i}$ represents the equilibrium sorption of the i th relaxation process. k_F represents as $4\pi^2 D / d^2$, where D is the diffusion coefficient and d is the particle diameter. This model provides a means for calculating a meaningful and useful diffusion coefficient from complex sorption data involving long term relaxations

which may overshadow the rapidly achieved Fickian diffusion. The model is also used to analyse the unexpected differences in sorption kinetics between experiments starting with penetrant-free samples (integral sorption) and those involving a finite initial penetrant concentration (incremental sorption).

Correlation of sorption with penetrant size

The density of the polymeric substance in the sorption centers is lower than that for the surrounding polymer , so that the centers may be considered as units of stable free volume present in the polymer (Gedraitite , 1988).

Thus , the free volume associated with the sorption centers corresponds to the maximum volume of a molecule which can be sorbed by this center.

Most of the usual organic compounds possess approximately the same density. Thus for each elementary unit of the free volume , there exist a certain maximum molecular weight of the compound sorbed by the center (Gedraitite et al. , 1989).

In each polymer , there must be a certain size distribution of the sorption centers , according to which the Langmuir sorption capacity of the polymer must decrease with increasing molecular mass of the penetrant under study. On the other hand , the energy of interaction of the

penetrant molecule with the polymer depends not only on the area of its contact with the polymer , which may be a function of the molecular mass of the penetrant , but also on a number of other factors , including the chemical nature of the penetrant and polymer , so that one cannot expect an unambiguous dependence of the sorption constants such as capacity factor and site affinity parameter on the molecular weight of the penetrant (Gedraitite , 1989). As previously described , one measure of molecular size is the constant b of the Van der Waals equation of state (Berens , 1975).

$$\left(P + \frac{n^2 a}{V^2} \right) (V - n b) = n R T \quad (24)$$

where b is the effective volume of the molecules in one mol of gas , in liter / mol.

MATERIALS AND METHODS

MATERIALS

Polymer Films

An amorphous polyamide , known as Nylon 6I / 6T , provided by the E.I. Dupont De Nemours and Co. was used for all studies. The polymer was synthesized from hexamethylenediamine and a mixture of isophthalic (70%) and terephthalic (30%) acids. Since the acid isomers were randomly placed into the polymer backbone , resulting in structural irregularity , no crystallization of the polymer matrix was observed. No evidence of crystalline melting point was found. A 1 mil thickness film was used for all studies. The volume fraction of n-propanol within the polymer as a function of vapor activity was measured by the density gradient technique (ASTM D 1505-68 , 1979).

n - Propanol

Used as a penetrant.

Supplied from Fisher Scientific Co., Pittsburgh , PA

Specific Gravity (at 25 ° C)	0.801
Molecular Weight	60.09 g / mol
Solubility	soluble in water and ether
Boiling Range	96.7 - 97.1 ° C
Purity	99.998 %

Dichlorobenzene

Used as a solvent for constructing a n-Propanol calibration curve.

Nitrogen

Used as a carrier gas. High purity dry nitrogen 99.98 % by the Union Carbide Corporation , Linde Division , Danbury , CT.

EXPERIMENTAL METHODS***Sorption measurements***

Equilibrium sorption studies were carried out using a Cahn Electrobalance , Model D 200 (Cahn Instruments Inc., Cerrito , California), which has a sensitivity of 10^{-7} g. A schematic diagram of the sorption apparatus is shown in Figure 3.

A constant concentration of n-propanol vapor was produced by bubbling nitrogen through the liquid n-propanol. The liquid n-propanol is contained in a vapor generator consisting of a Pyrex glass gas washing bottle , 250 mm long and 50 mm diameter, with a frittered dispersion tube. The organic vapor stream can then be mixed with another source of pure nitrogen , if further dilution is needed.

Before actual testing was conducted, rotameter settings were determined to provide a range of vapor activities. Vapor activity was calculated by dividing the experimentally determined vapor pressure by the saturated vapor pressure (Perry Handbook.). Figure 4 is the saturated vapor pressure curve of n-propanol plotted as a function of temperature.

Rotameters were used to provide an indication of the settings required for the desired vapor activities. The gas flows to the rotameters were regulated by Nupro "M" series needle valves. The relationship between the rotameter settings and vapor activities is described in Table 2. Each value of the rotameter column in Table 2 indicates the rotameter reading, when the middle zone of a spherical bead inside the rotameter is aligned with the rotameter calibration line. Digital mass flowmeters were also incorporated between the dispensing manifold and the test cell (inside sampling port), to provide a continuous indication that a constant rate of flow was maintained.

As shown in Figure 3, two sampling ports were installed, both inside and outside the chamber, to determine accurately the vapor activity within the hangdown tube, which contained the film sample. Table 2 also shows the difference in vapor concentration between the two sampling port locations.

For the calculation of vapor activity, a standard calibration curve for n-propanol was prepared. A detailed procedure and data are presented in Appendix A and Figure 5, respectively. A Hewlett Packard 5890A gas chromatograph equipped with dual flame ionization detection, interfaced to

a 3390A GC Hewlett Packard terminal was used for propanol detection. The 5890A GC is a keyboard controlled instrument with a multifunctional digital processor. From the digital processor, the area under the peak and retention time was obtained.

Before starting a run, a film sample, $1\frac{1}{4}$ "W x $3\frac{1}{2}$ "L, and approximately 100 mg weight was cut from the sample roll and dried in the vacuum oven (24 hours, 70°C , 30 psi). The dried film sample was transferred quickly into the hangdown tube of the electrobalance which is installed inside a constant temperature chamber (Thermotron Model SM-32S-SH, Thermotron Industries, Holland, Michigan). The film sample was suspended directly from the arm of the electrobalance, and the system purged with nitrogen until a constant weight was attained. This process was monitored by computer screen display. Figure 6 is a graphical display of a typical sample weight profile prior to initiating the sorption run.

Care must be taken to calibrate the electrobalance prior to performing sorption experiments. Appendix B provides a brief description of the procedure for electrobalance calibration.

When the sample weight change during the purging process reached a constant value the sorption experiment test was initiated, starting with the lowest vapor activity. This was accomplished by careful control of the rotameter settings (Vapor and Nitrogen), whose values were predetermined (Table 2). Sorption data was compiled on a computer disc at one hour

intervals. Simultaneously the sorption procedure was followed on the monitor screen through a linear graph , which enables continuous monitoring of the sorption process.

The sorption of n-propanol was measured at 23 ° C by the successive sorption or interval sorption method (Bagley and Long , 1955).

For interval sorption studies , the film sample was permitted to equilibrate with the propanol vapor of fixed vapor activity.

When the sorption reached the equilibrium state , the vapor activity was quickly changed to the next level (a), and the same procedure repeated until sorption data values for the highest vapor activity were obtained. During each sorption experiment , the vapor activity was checked twice daily to insure a constant sorbate concentration throughout the course of the experiment. Appendix C shows the fluctuation of vapor activity in each stage.

Density experiments

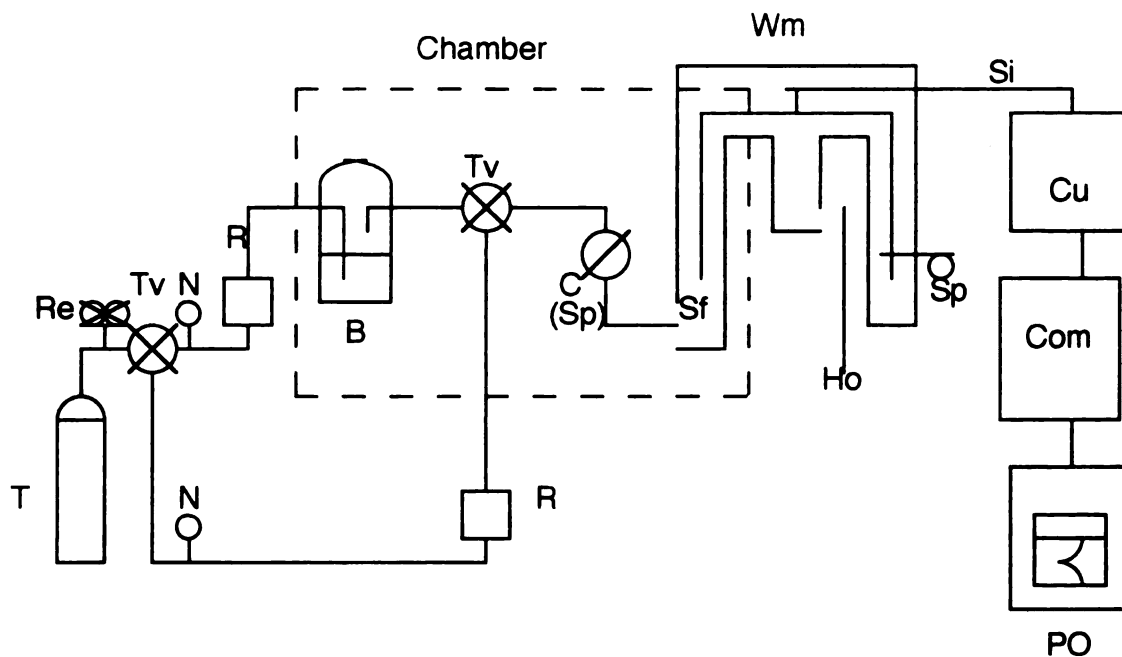
The test procedure followed was in accordance with the ASTM D 1505 (Standard test method for Density of Plastics by the Density Gradient Technique).

Film densities were determined in a density gradient column with the

gradient made of toluene and carbon tetrachloride , which have densities of 0.87 and 1.59 respectively.

For the gradient tube preparation , method C(ASTM D 1505 Appendixes A 2.3) was adopted where the liquid entering the gradient tube becomes progressively more dense. Care should be taken to fill up the density gradient tube with toluene and carbon tetrachloride mixtures , since the calibration floats would not be placed correctly unless the filling procedure is performed at a slow enough rate (approximately 30 min / 300 mm length of column).

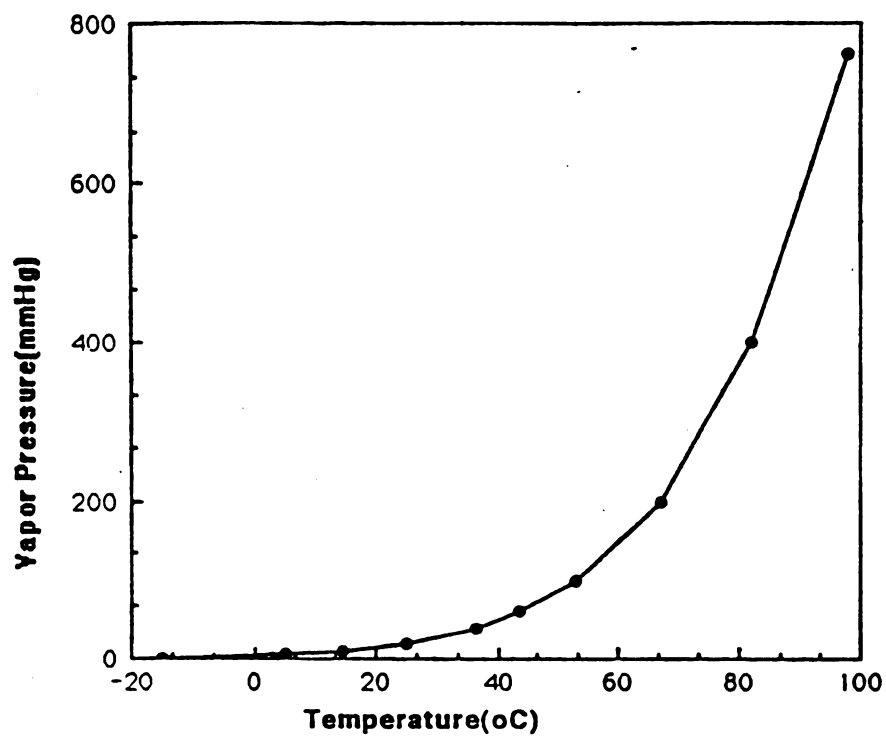
Test samples whose change in density on conditioning may be greater than the accuracy required of the density determination should be conditioned before testing in accordance with the method listed in the applicable ASTM material specification.



B : Organic vapor Bubbler
 Ch : Temperature constant
 Chamber
 CU : Control Unit (By
 Computer
 C : Cell for sampling (Vapor
 activity check)
 COM:Computer
 Ho : Hood
 N : Needle Valve

R : Rotameter
 PO: Plotter
 Re: Regulator
 Sf: Sample film
 Si: Electric signal
 Sp: Sampling pot
 T : Nitrogen Tank
 Tv: Three way Valve
 Wm: Cahn Electrobalance
 (D200-02)

Figure 3. Schematic diagram of the electrobalance test apparatus



$$y = 3.1970 + 0.27732x + 1.0137e-2x^2 + 1.2757e-4x^3 + 3.0759e-6x^4 + 2.5935e-8x^5 \quad R^2 = 1.000$$

Figure 4. Saturated Vapor Pressure of n-Propanol

(using polinomial # 5)

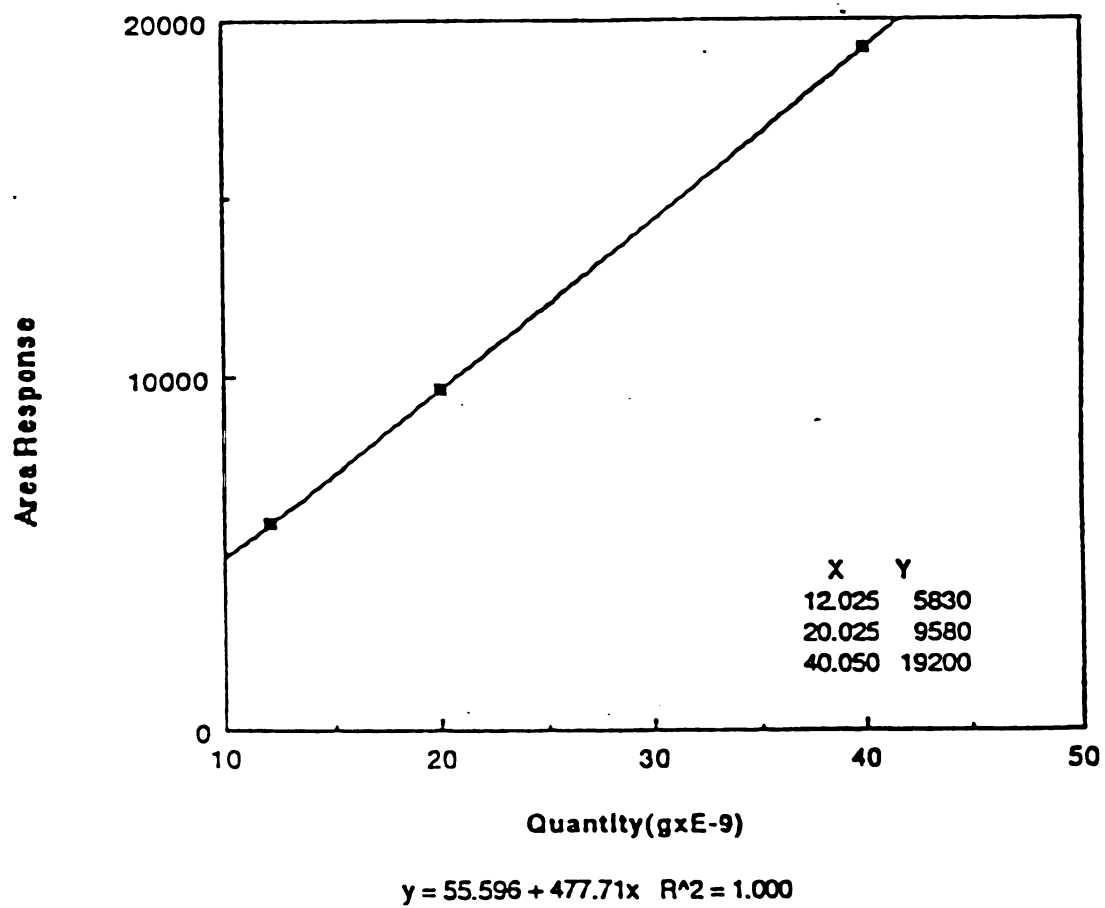


Figure 5. Standard calibration graph of n-propanol at 23 °C

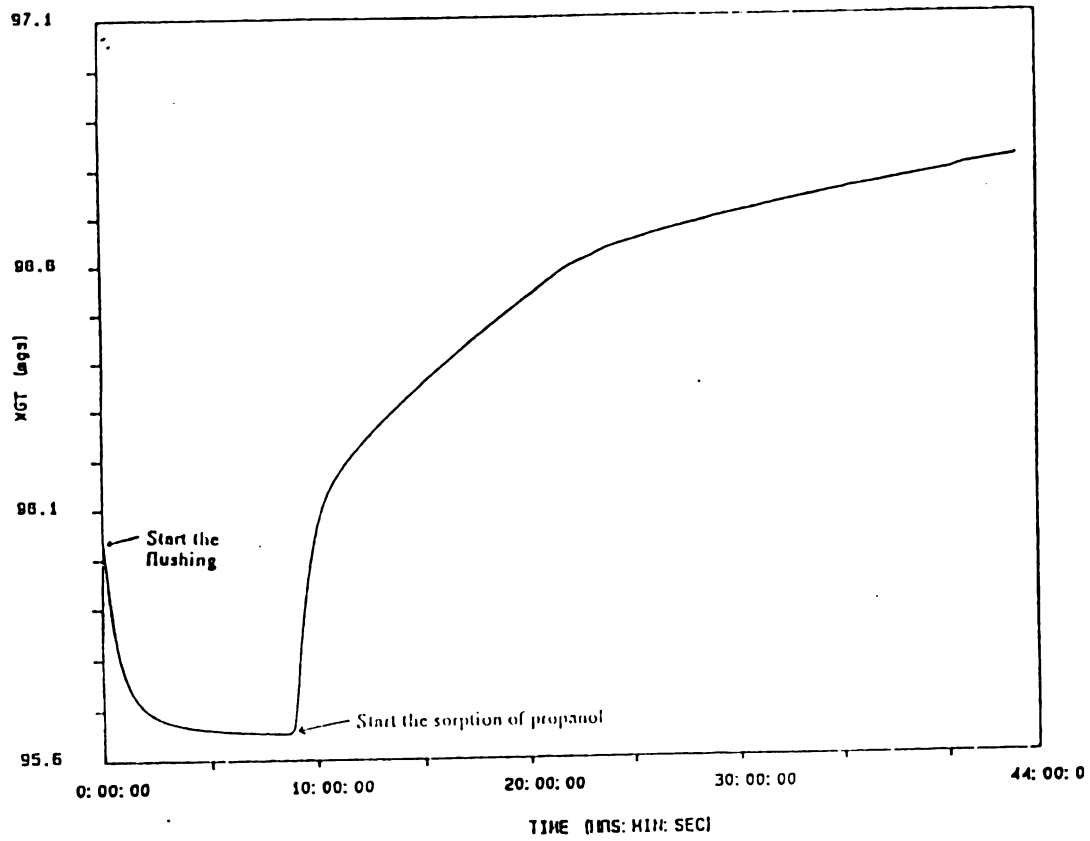


Figure 6. Illustration of sample flushing by nitrogen at 23 °C

No	Rotameter vapor N ₂		Inside sampling port				Outside sampling port			
			A.R	a	X	S.D	A.R	a	X	S.D
1	0.5	55	1.129xE6	.0203			1.145xE6	.0207		
			1.2015	.0217	.021	.0008	1.1459	.0207	.021	.0003
			1.1804	.0213			1.1293	.0204		
			1.1003	.0199			1.1705	.0211		
2	1	50	1.466xE6	.0265			1.253xE6	.0226		
			1.725	.0311			1.503	.0271		
			1.681	.0303	.029	.0026	1.453	.0262	.027	.0020
			1.373	.0248			1.488	.0269		
			1.718	.0310			1.558	.0281		
			1.573	.0284			1.581	.0286		
3	1	40	2.442xE6	.0441			2.229xE6	.0402		
			2.5586	.0462	.046	.0012	2.4556	.0443	.043	.0027
			2.5648	.0463			2.5141	.0454		
4	2	50	2.74xE6	.0495			2.62xE6	.0473		
			2.824	.0510	.051	.001	2.7274	.0492	.048	.0026
			2.8418	.0513			2.6359	.0476		
5	5	50	4.78xE6	.0864			4.84xE6	.0873		
			4.9522	.0895	.087	.0037	4.8783	.0881	.088	.0008
			4.5309	.0818			5.1716	.0934		
			4.9841	.0899			4.534	.0819		
6	7	50	5.65xE6	.1021			5.74xE6	.1036		
			5.8577	.1058	.102	.0029	5.5998	.1011	.099	.0042
			5.5078	.0995			5.4223	.0979		
			5.5406	.1000			5.2013	.0939		
7	15	40	1.58xE7	.2856			1.59xE7	.2883		
			1.5723	.2848			1.6972	.3074		
			1.5198	.2753	.287	.0091	1.5124	.2739	.287	.0184
			1.6611	.3008			1.4522	.2630		
			1.5794	.2859			1.6613	.3009		

Table 2. Relationship between rotameter readings and vapor activities

RESULTS AND DISCUSSION

Data preparation and preliminary test

All sorption experiments of n-propanol in Nylon 6I/6T were determined at 23 ° C. Prior to carrying out the sorption studies, several parameters which were related to the sorption measurements were determined.

These include :

- (1) Calibration curve for n-propanol vapor to calculate the vapor concentration levels was prepared (see Figure 5). The detailed procedure is described in Appendix A.
- (2) The relationship between the rotameter settings and vapor activities at the inside and outside sampling port was determined and presented in Table 2. This results showed good agreement between the vapor activity values with an error of 6 %.
- (3) Dried film samples, which were quickly transferred from the vacuum oven to the hangdown tube showed a weight loss during the purge step which was assumed to be due to rapid moisture uptake during sample transfer to the sorption system.

It was found that to insure complete drying , it was necessary to wait at least 5 or 6 hours after the film sample attained a constant weight to initiate sorption studies. The initial sorption experiment was then started by adjusting the rotameters (N₂ , vapor) to predetermined values. Figure 6 illustrates the weight change of the polymer film sample, following purging the electrobalance hangdown tube with dry nitrogen gas.

- (4) Saturated vapor pressure of propanol at 23 ° C was calculated as 17.52 mmHg from the equation in Figure 4.

In accordance with the above considerations , preliminary studies were also carried out using two separate film samples in order to evaluate the reproducibility of the sorption experiment. Initial sorption studies were carried out under the condition of vapor activity $a=0.06$, and repeated with a second film sample without changing test conditions. Sorption profile curves are presented in Figure 7. As shown, good reproducibility was obtained between the two runs with an error less than 3%, which proves that the apparatus was reliable.

Over the course of the entire experiment , vapor activities were carefully monitored , and the results are summarized in Table 4 and presented graphically in Figures 29 to 37, in Appendix C. Plots show the scatter band of vapor activities versus time and , each data point represents the average value of four or five replicate analysis at the corresponding time interval. Vapor activity fluctuation did not exceed $\pm 7 \%$ throughout the course of the studies.

Equilibrium Sorption

The sorption of n-propanol in Nylon 6I / 6T , as a function of vapor activity was determined at 23 ° C. Figures 8 to 16 present the weight gained for each successive interval sorption measurement, where the uptake mass fraction is plotted as a function of time.

Figure 17 shows the overall sorption profile , that includes the experiments carried out over the entire vapor activity range (i.e. 0.035-0.91). This figure indicates that "true" equilibrium was obtained within a period of time less than 20 hours , for n-propanol vapor activity below 0.11.

As shown in Figures 12 to 16 , above a vapor activity of 0.11 , the sorption process for the propanol / Nylon 6I / 6T system appears to be best described by the diffusion - relaxation model proposed by Berens and Hopfenberg (1977) , who interpreted the sorption mechanism of vinyl chloride monomer by polyvinyl chloride as following a Fickian diffusion process at the low vapor activity levels , and an anomalous relaxation process at the high vapor activity levels.

As shown in Figure 18 , for n-propanol activity levels $a < 0.11$, the sorbate uptake was very rapid and the sorbate / polymer system attained equilibrium conditions. This process can be described as Fickian , where the diffusion coefficient is a function of vapor concentration , but is not time dependent.

Analysis of sorption behavior at vapor activity below 0.11

As shown in Figure 18 , when the interval between the initial and final concentration , C_i and C_f is small , equilibration times of less than 10 - 12 hours were observed for the Fickian diffusion process. Thus , the Fickian diffusion pathway may be assumed to be essentially completed before applicable stress - relaxation has occurred. This suggests that the concentration differential is not a variable that determines whether the process is Fickian , but rather the level of vapor concentration determines sorption behavior. Above $a = 0.11$ the sorption process is not Fickian and exhibits anomalous behavior, while the sorption process appears to follow Fickian behavior at vapor activities $a < 0.11$. The limited amount of sorption data , excludes any possibility of fitting the data to the Langmuir-Flory-Huggins model , over the whole range of vapor activity. However , the data obtained at a vapor activity below 0.11 can be modelled.

As shown in Figure 19, a plot of the weight fraction as a function of vapor activity shows a linear relationship. Where the weight fraction (W_f) is defined as the weight gain over the total sample weight

$$W_f = \frac{W_s}{W_s + W_p} \quad (25)$$

Where W_s is the mass of the sorbate and W_p is the mass of the sample.

This can be interpreted in two ways ; (i) a simple Henry's law is applicable , which suggests simple dissolution of n-propanol in the polymer film at the low vapor activity levels ($a < 0.11$) , or (ii) the Langmuir-Flory-Huggins model can be applied at low concentration levels since the Flory-

Huggins equation is quasi-linear at low vapor activity levels and the Langmuir equation (see Equation (1)) can also be simplified by reducing the denominator $1 + bp$, where it is assumed that $bp \ll 1$ at low vapor activity levels ($a < 0.11$), and

$$C = C'_H p \quad (26)$$

From Equation (15), for a range of activity values from 0 to 0.11 and an assumed λ value of 1.6, a theoretical plot can be obtained which illustrates the linearity of the Langmuir-Flory-Huggins model. The calculated data and the associated plot are presented in Table 3 and Figure 20 respectively.

However, this approach to modelling the sorption process for the n-propanol / Nylon 6I/6T system could not be verified due to the lack of data points and the extraordinary amount of time needed to complete the studies.

Figure 20 represent the relationship between volume fraction and vapor activity at the low vapor activities ($a < 0.11$). Similar to Langmuir plots of P / C_H versus P , the straight line in Figure 20 gives clear evidence of a Langmuir type sorption model for the sorption of n-propanol by Nylon 6I/6T, at the low vapor activities. From the sorption studies diffusion coefficients can be determined, when sorption levels are at the equilibrium state. The M_t / M_∞ vs $t^{1/2}$ curves for the low vapor activities are presented in Figure 21 to 24. The sorption diffusion coefficient (D_s) was then calculated from Equation 22 by setting M_t / M_∞ equal to 0.5 and solving t give D_s . As the sorption uptake levels were measured by hours, the diffusion coefficient value might have some inherent errors.

Figure 25 presents a comparison between experimental and calculated data for an independant integral sorption experiment carried out at $a = 0.035$. Good agreement was obtained at the low vapor activities whereas significant differences between the experimental and calculated curves were obtained at

the high vapor activities, this can be explained as Fickian diffusion at the low vapor activities and time dependent diffusion by relaxation - controlled swelling at the high vapor activities.

Volume fraction (V_1)	Vapor activity
0.002	0.027
0.003	0.040
0.004	0.053
0.005	0.066
0.006	0.079
0.007	0.092
0.008	0.104
0.009	0.117
0.010	0.129

Table 3. Volume fraction vs. vapor activity from Flory-Huggins equation
 $\ln a_1 = \ln V_1 + V_2 + \chi V_2^2$ when $\chi = 1.6$, $V_1 = 1 - V_2$

Step	Average vapor activity	Standard deviation
1	0.035	± 0.003
2	0.050	± 0.0016
3	0.080	± 0.0042
4	0.110	± 0.003
5	0.295	± 0.0069
6	0.390	± 0.0084
7	0.490	± 0.015
8	0.840	± 0.027
9	0.910	± 0.0046

Table 4. Average vapor activity and standard deviation for each successive vapor activity interval

Analysis of sorption behavior at vapor activities above 0.11

A somewhat similar "two stage" sorption process has been observed by Bagley and Long (1958) for the sorption of acetone by ethyl cellulose and by Fujita (1961) for several other systems. Berens and Hopfenberg (1977) also observed a two stage sorption process as previously discussed.

The "two stage" sorption process can be discussed as follows:

when a solid polymer is brought into contact with a penetrating vapor , the penetrant diffuses into the polymer and the polymer swells. Swelling of the polymer involves larger scale segmental motion resulting , ultimately , in an increased distance of separation between polymer molecules and it shows a long term relaxation. This interpretation also seems to be applicable to the n-propanol / amorphous polyamide system ; in the early stage of sorption , the n-propanol concentration gradient provides the major driving force and the transport process is dominated by the Fickian diffusion (Figure 8 - 11).

When the concentration of n-propanol resulting from this process is sufficient to develop a significant swelling stress , the slow response of the glassy polymer to this stress produces gradual swelling of the amorphous polyamide structure and permits additional sorption (Figure 12 - 16). This swelling-relaxation process may continue even after the Fickian process has produced a virtually uniform concentration of propanol through the amorphous polyamide.

In this event , the sorbate concentration resulting from Fickian diffusion becomes negligible , and the later stage of sorption is dominated by the relaxation - controlled process (Berens , 1977).

As discussed above , a distinct two stage sorption process was observed at the high vapor activities ($a_1 > 0.11$). The rate of sorption in the initial stage is principally controlled by the Fickian process and therefore, may be used to estimate a true diffusion coefficient, even when the total sorption does not follow the Fickian model (Berens , 1977) .

Furthermore , since the second sorption stage is almost entirely relaxation - controlled , the kinetic and equilibrium parameters describing the slow relaxation process can be obtained from long time sorption data.

To determine if the initial portion of the sorption profile , which exhibited "two stage" sorption behavior , followed Fickian behavior , and to estimate the diffusion coefficient the following treatment was applied with the aid of a computer - assisted fitting routine.

Initially , values of M_∞ were intuitively selected by inspection of a plot of the experimental M_t vs. t data. This is illustrated for sorption studies discribed in Figure 26, as shown, the M_∞ value for a Fickian diffusion process is assigned , the $t^{1/2}$ value can be obtained from a plot of M_t / M_∞ versus $t^{1/2}$ (Figure 27) and the diffusion coefficient (D_s) calculated by solution of equation (22).

By substituting the D_s value into Equation (21) , calculated values of M_t are obtained.

The calculated and experimental values of M_t / M_∞ versus $t^{1/2}$ are then plotted and the quality of the fit is evaluated by graphical analysis.

If the experimental and calculated values show poor agreement , this

procedure is repeated with a new value of M_{∞} until a satisfactory fit between the calculated and experimental values is obtained (Figure 26).

As shown in Figure 28, an assigned value of $M_{\infty} = 0.275$, gave good agreement (Figure 28) between the experimental and calculated data for the sorption profile plot at $a = 0.295$. The estimated diffusion coefficient for the initial stage of the sorption profile (i.e, Fickian) was $1.264 \text{ E-}10 \text{ cm}^2/\text{sec}$.

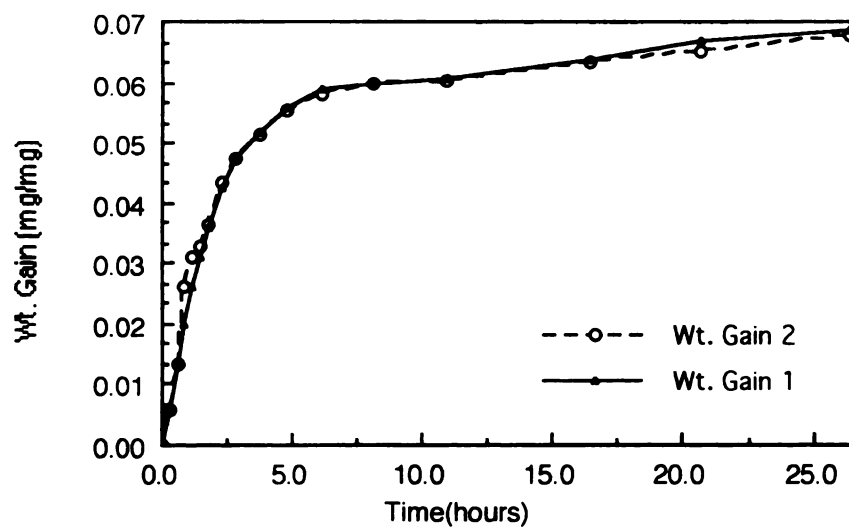


Figure 7. Evaluation of the reproducibility of the sorption system at $a = 0 - 0.06$

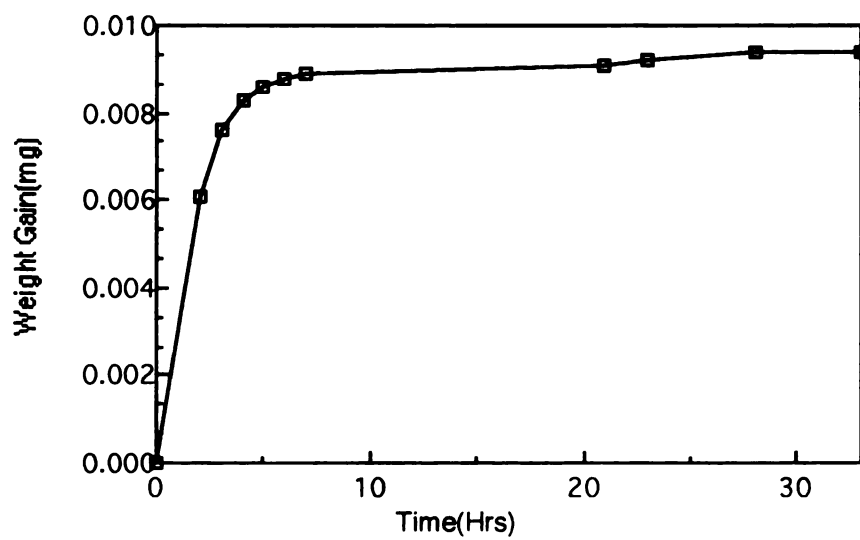


Figure 8. Interval sorption of n-propanol at $a = 0 - 0.035$

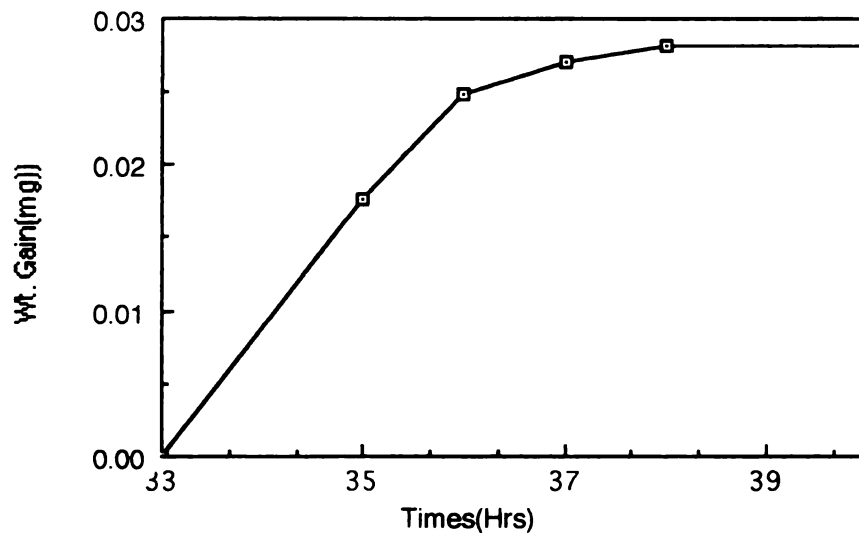


Figure 9. Interval sorption of n- propanol at $a = 0.035 - 0.050$

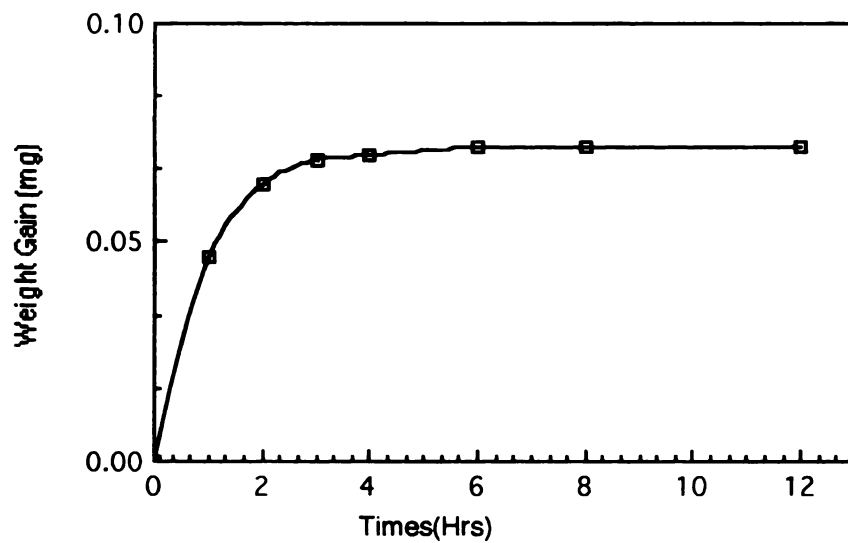


Figure 10. Interval sorption of n- propanol at $a = 0.050 - 0.080$

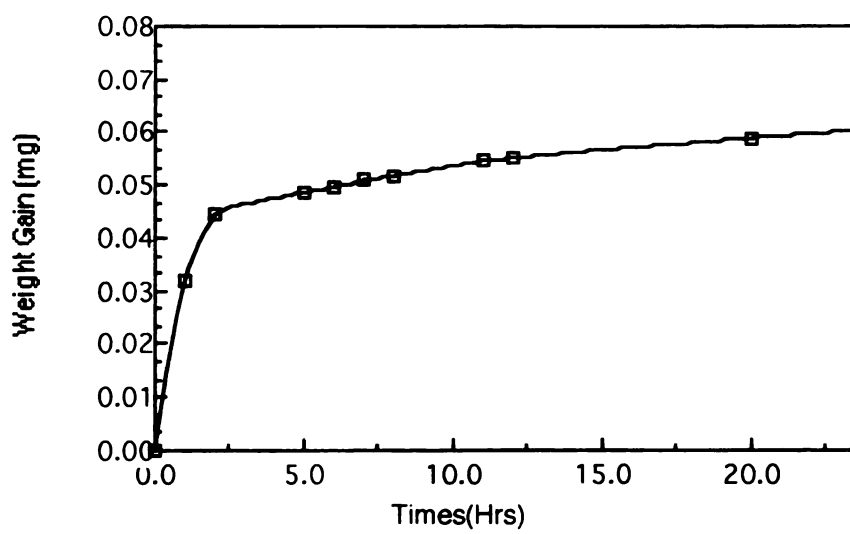


Figure11. Interval sorption of n- propanol at $a=0.080-0.110$

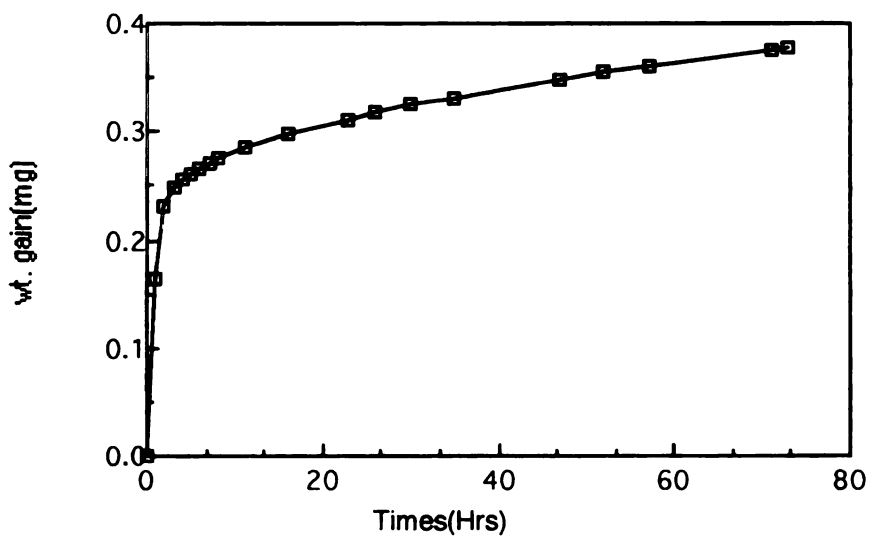


Figure12. Interval sorption of n- propanol at $a=0.11-0.295$

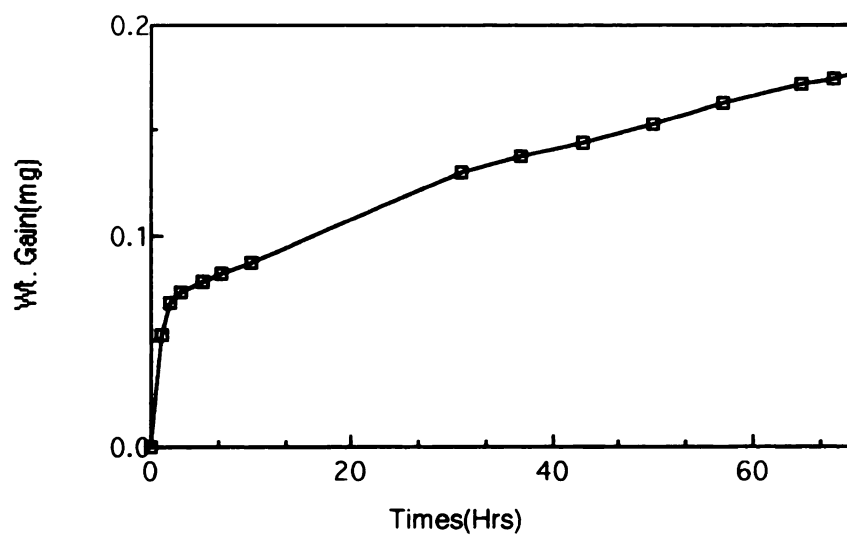


Figure13. Interval sorption of n- propanol at $a=0.295-0.390$

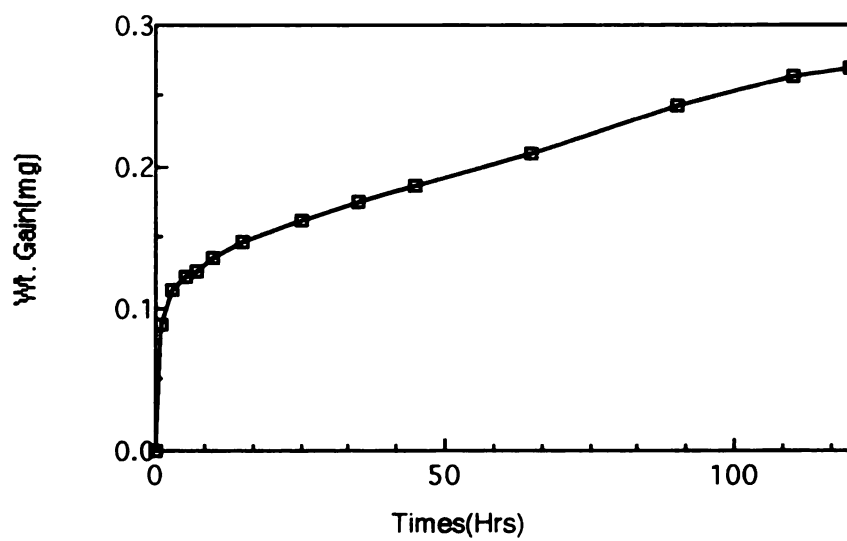


Figure14. Interval sorption of n- propanol at $a=0.39-0.490$

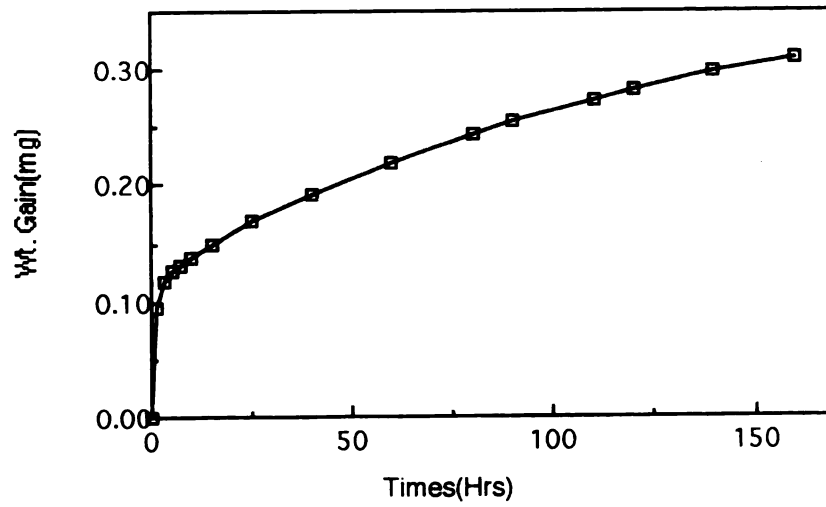


Figure15. Interval sorption of n- propanol at $a=0.49-0.840$

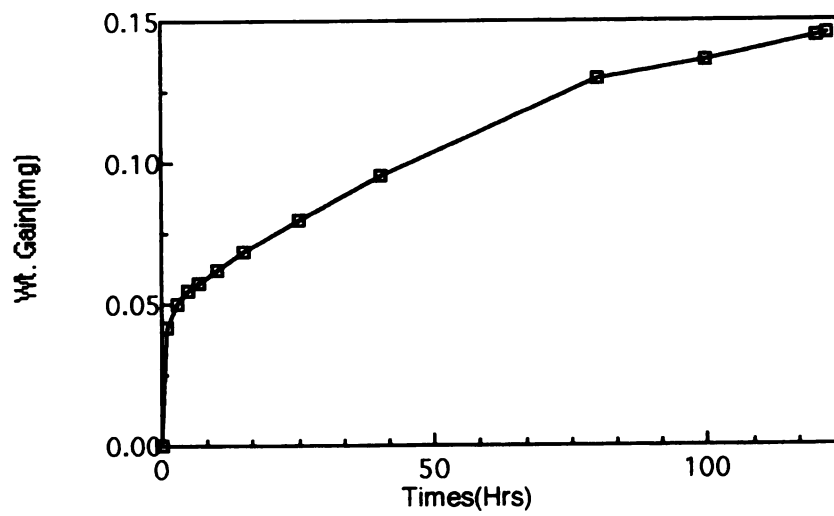


Figure16. Interval sorption of n- propanol at $a=0.84-0.910$

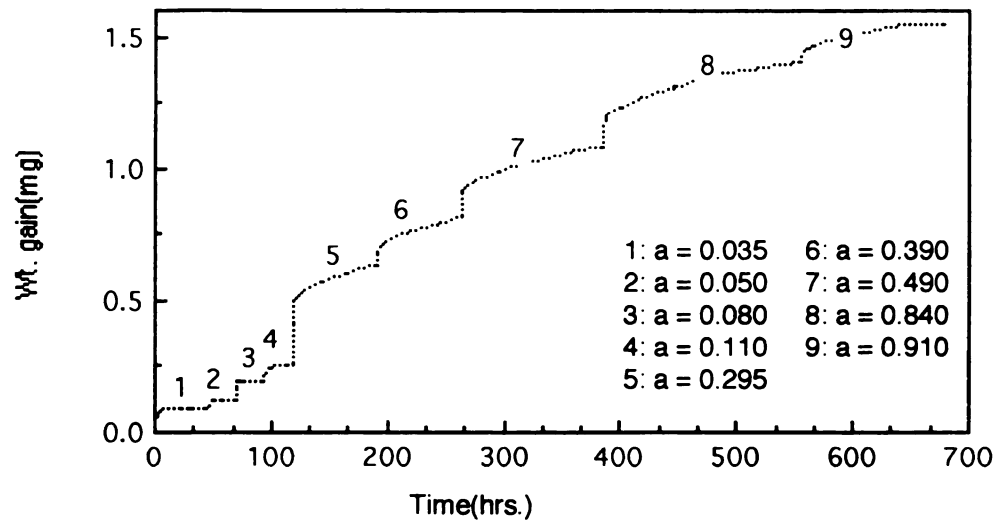


Figure 17. Successive interval sorption of n- propanol into Nylon 6I/6T at 23 °C ($a = 0 - 0.91$)

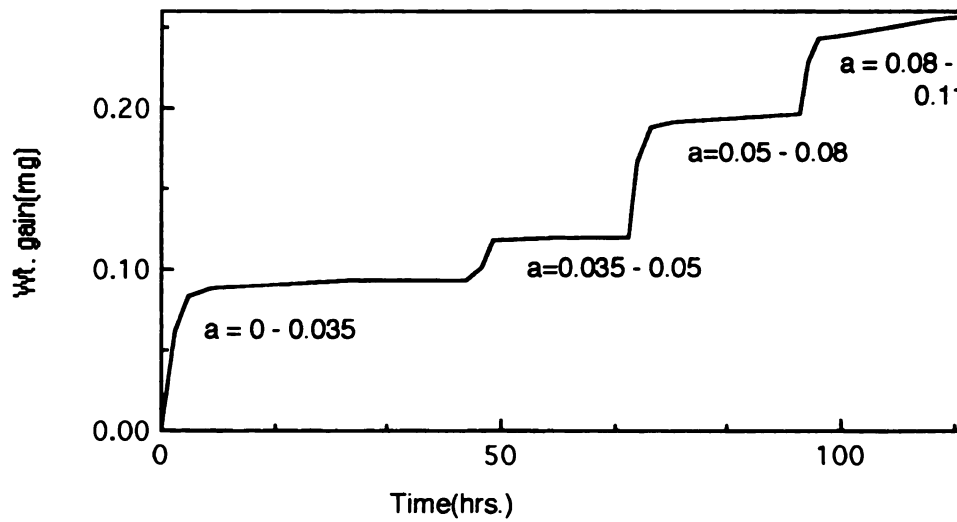


Figure 18. Successive interval sorption of n- propanol into Nylon 6I/6T at 23 °C ($a = 0 - 0.110$)

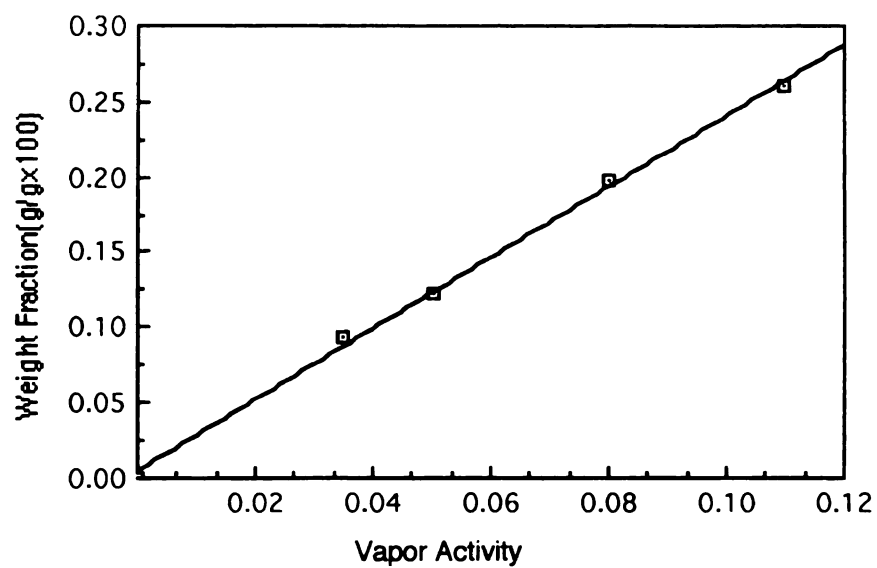


Figure 19. Experimental sorption isotherm for propanol in Nylon 6I/6T at low vapor activities ($a < 0.11$)

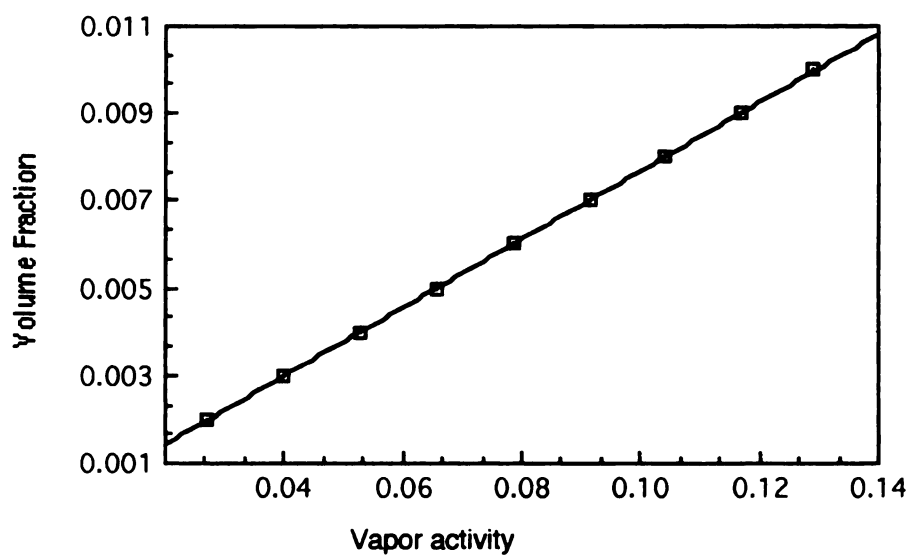


Figure 20. Flory-Huggins plot when $l = 1.6$, from the equation $\ln a = \ln V_1 + V_2 + V_2$

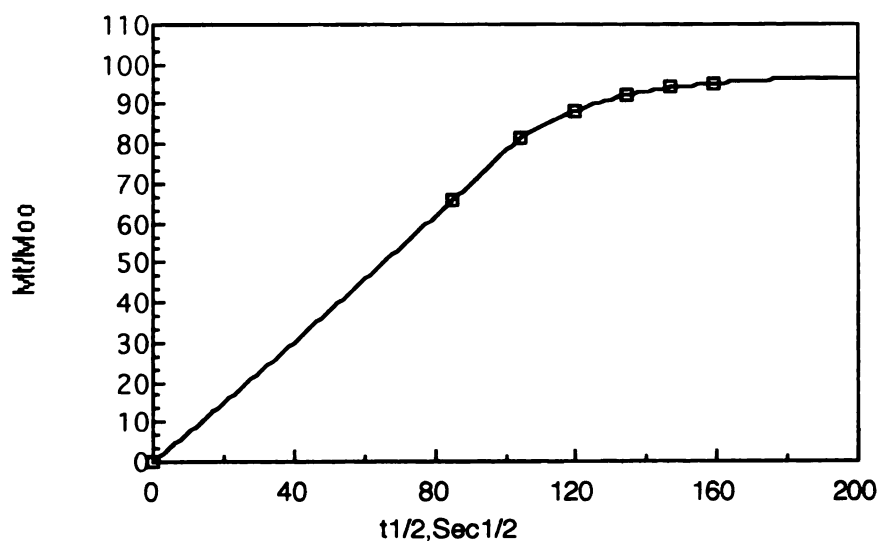


Figure 21. Plot of M_t/M_{∞} vs $t_{1/2}$ for n- propanol sorption by Nylon 6I/6T, at 23 oC ($a = 0.0 - 0.035$)

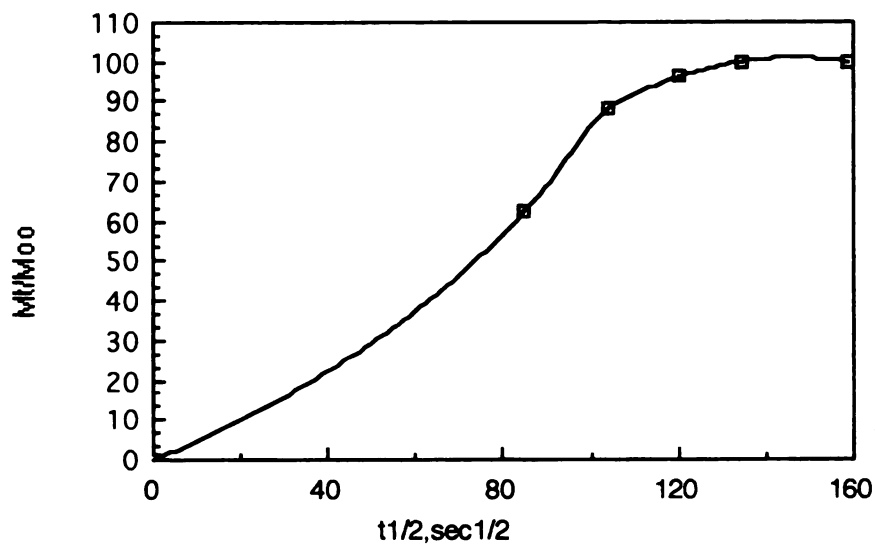


Figure 22. Plot of M_t/M_{∞} vs $t_{1/2}$ for n- propanol sorption by Nylon 6I/6T, at 23 oC ($a = 0.035 - 0.050$)

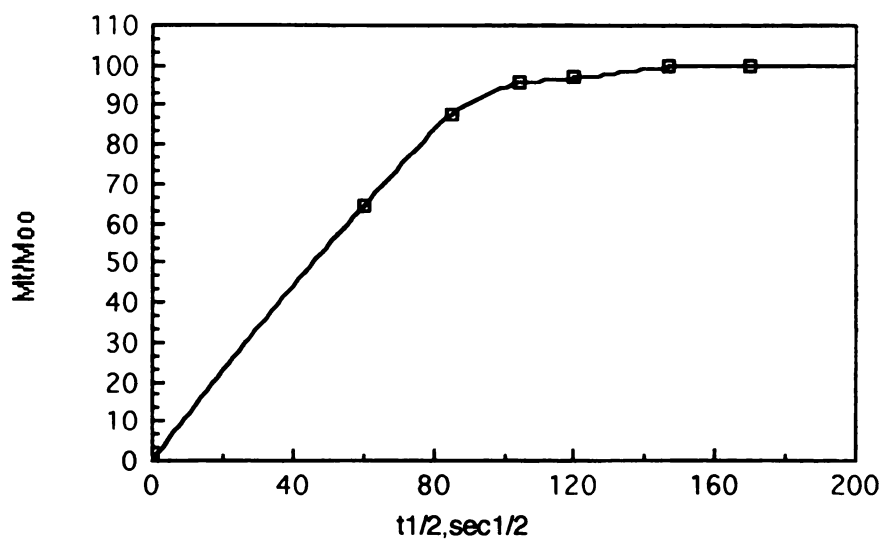


Figure 23. Plot of M_t/M_{∞} vs $t^{1/2}$ for n- propanol sorption by Nylon 6I/6T, at 23 oC ($a = 0.05 - 0.08$)

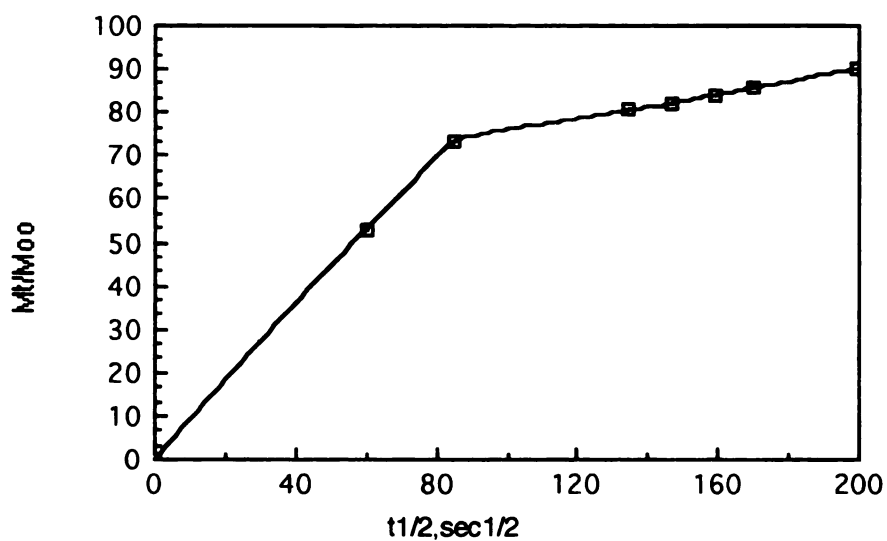


Figure 24. Plot of M_t/M_{∞} vs $t^{1/2}$ for n- propanol sorption by Nylon 6I/6T, at 23 oC ($a = 0.08 - 0.11$)

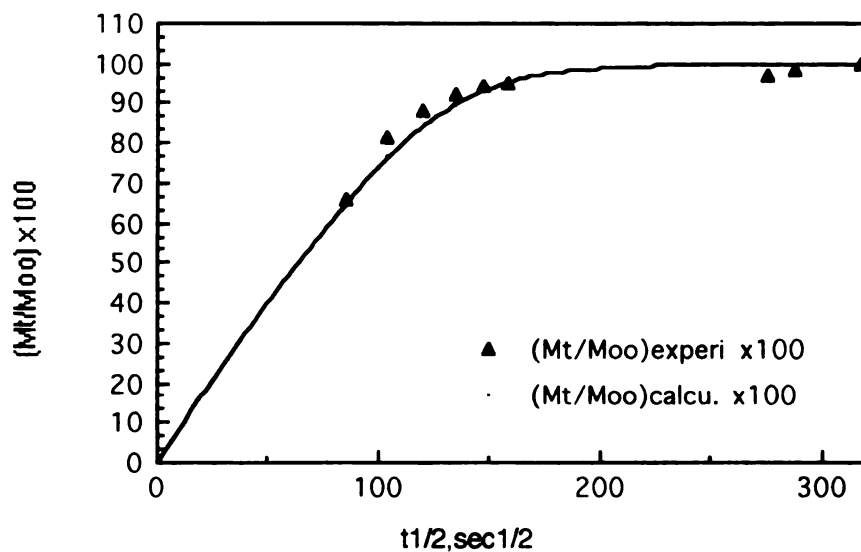


Figure 25. Comparison between experimental and calculated data at vapor activity $a = 0.035$

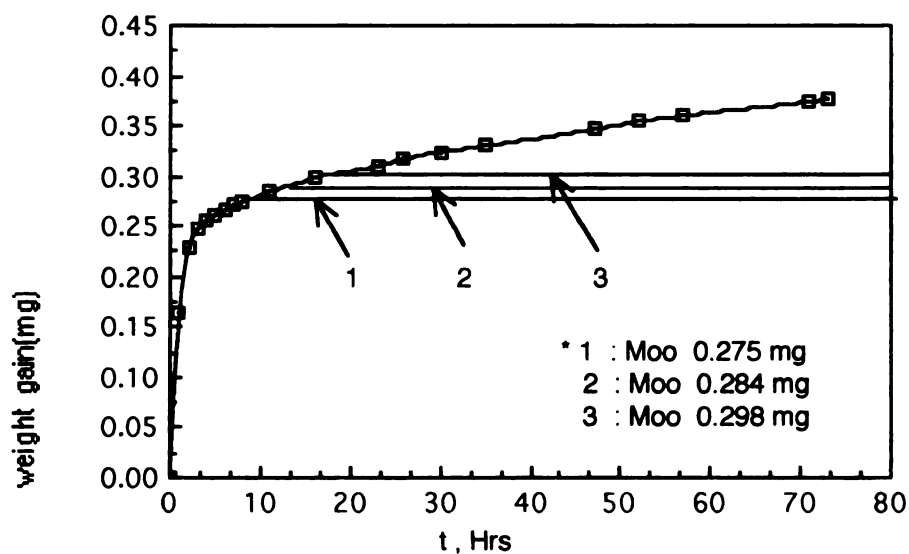


Figure 26. Deviation from Eqn.(21) due to non-Fickian sorption for sorption of propanol by Nylon 6I/6T at 23°C ($a=0.11-0.295$): Graphical Estimation of Fickian M_{∞} value

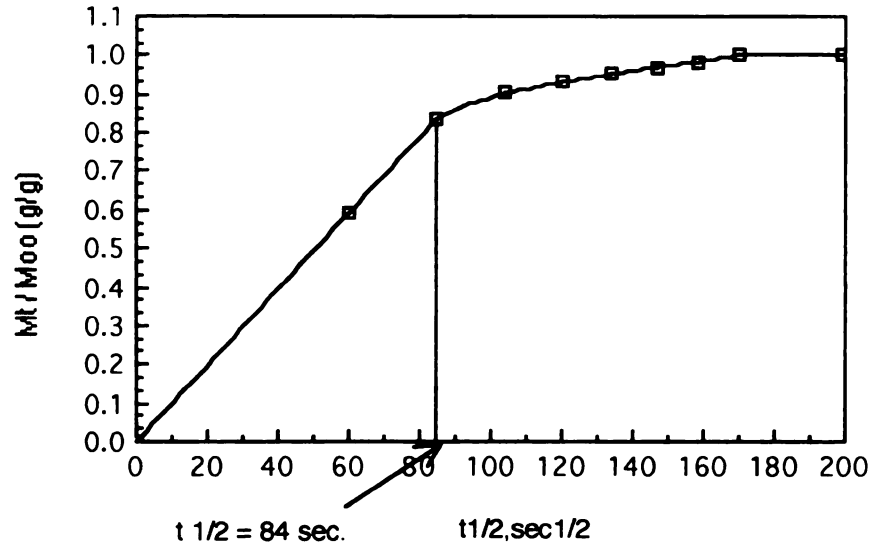


Figure 27. Plot of M_t/M_{∞} vs. $t_{1/2}$ for n- propanol sorption by Nylon 6I/6T, 23 oC, $a = 0.11 - 0.295$, Eqn.(21) for $M_{\infty} = 0.275$ and $t_{1/2} = 84$ sec.

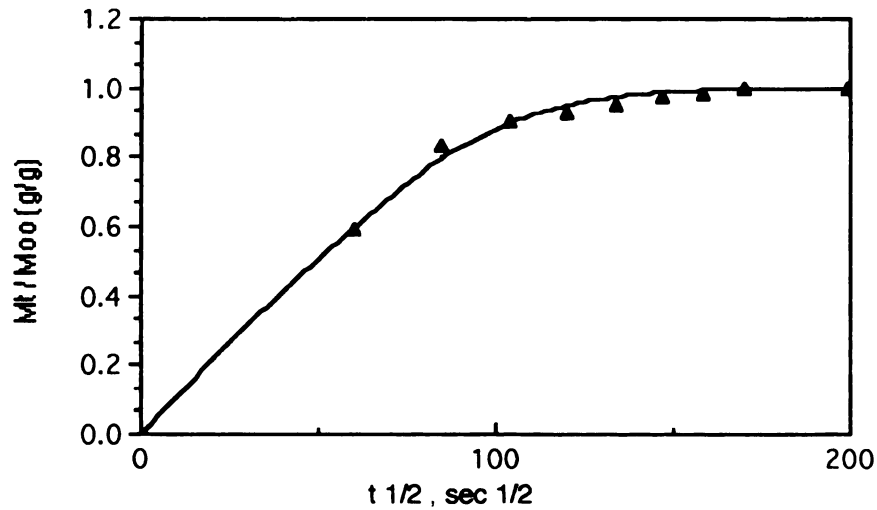


Figure 28. Plot of M_t/M_{∞} vs. $t_{1/2}$ for n- propanol sorption by Nylon 6I/6T, 23 oC ($a = 0.11 - 0.295$): point observed, curve, Eqn.(21) for $M_{\infty} = 0.275$ and $t_{1/2} = 84$ sec.

Conclusion

The sorption of propanol by amorphous polyamide, evaluated by an incremental sorption technique, showed that simple Fickian kinetics were obeyed and equilibrium was achieved within a short time at very low vapor activities ($a_1 < 0.11$). However, at high activity levels ($a_1 > 0.11$), the initial, rapid sorption was followed by a slower further uptake of propanol, which was qualitatively attributed to a relaxation-controlled swelling process. The initial rapid stage of sorption may be related to the Fickian diffusion of penetrant into pre-existing and available vacancies or sites in the glassy polymer. The relaxation processes, which occur over a long time scale may be related to a structural reordering or redistribution of free volume elements to provide additional sites of suitable size and accessibility to accommodate more penetrant molecules.

Appendix A

Procedure of standard calibration curve construction

In all cases , a standard curve of response vs. penetrant concentration was constructed from standard solutions of known concentration.

Calibration solutions were prepared by dissolution of known quantities of n-propanol in dichlorobenzene. The detailed procedure follows:

1. Bake out vials and syringes in oven prior to use to remove any residual solvent or permeant. Cool to room temperature.
2. Using the gas chromatograph , check the retention time of each solvent by head space technique to ensure there is no interfering peaks at the propanol retention times.
3. Prepare dilute solutions for the permeant standards by the following procedure:
 - fill up 100 ml volumetric flask with 10 μ l of n-propanol and dilute to make with dichlorobenzene. This becomes 100 ppm standard solution.
 - make up similar standard solution with dichlorobenzene , which becomes a standard solution of 50 ppm concentration.
 - Make 2 or 3 more different concentration solutions by using the same method
4. From the lowest concentration solution , inject 0.5 μ l sample solution directly into the gas chromatograph and the area response recorded.

Replicate the run and calculate the average

5. Plot the gas chromatograph area unit response vs. the number of grams injected per sample. The slope of this curve equals the calibration factor. Injected quantity can be calculated as follows

$$W = \text{concentration(v/v)} \times 0.5 \mu\text{l} \times 1 \text{ ml}/1000 \mu\text{l} \times \text{propanol density(g/ml)}$$

6. Setting conditions of gas chromatograph are as follows :

- o Oven temp. : 50 ° C
- o Initial time : 5 min.
- o Rate : 3 ° / min.
- o Final time : 0 min.
- o Final temp. : 165 ° C
- o Inject temp.: 200 ° C
- o Detect temp.: 250 ° C
- o Oven max. : 250 ° C
- o He carrier gas : 33 ml/min.
- o Sample injected : 0.5 μl
- o Head space test : 100 μl inject
- o Concentration used : 100 , 50 , 25 , 10 , 5 ppm (5 kinds)

Appendix B

Electrobalance Calibration Procedure

Cahn D-200 Electrobalance can be calibrated by the following procedure.

1. Suspend the sample container on the hangdown wire
2. Press the down arrow key three times and the NET WEIGHT box will display the weight that the balance is actually seeing.
3. Enter "Y" into the REZERO box. Next, press the up arrow key once to go back to the Balance Calibrate menu.
4. Enter into Tare Balance box "Y" and the balance will tare.
5. Press the down arrow key to input the calibration weight
6. Remove the hangdown tube so that the pan is exposed. Then put the 100 mg calibration weight onto the sample weight pan. Replace the hangdown tube for stable reading.
7. Place the cursor into the Calibrate Balance box and enter "Y" and press ENTER when the pan with the calibration weight is steady.
8. Lower the hangdown tube and remove the calibration weight.
9. Suspend the sample and set up run conditions.

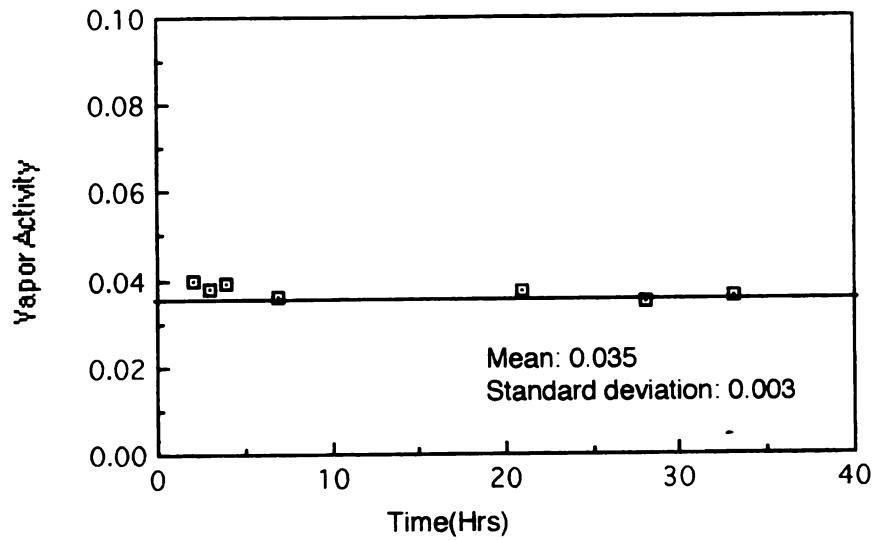
Appendix C.**Vapor activity fluctuation**

Figure 29. Distribution of vapor activity at $a = 0.035$

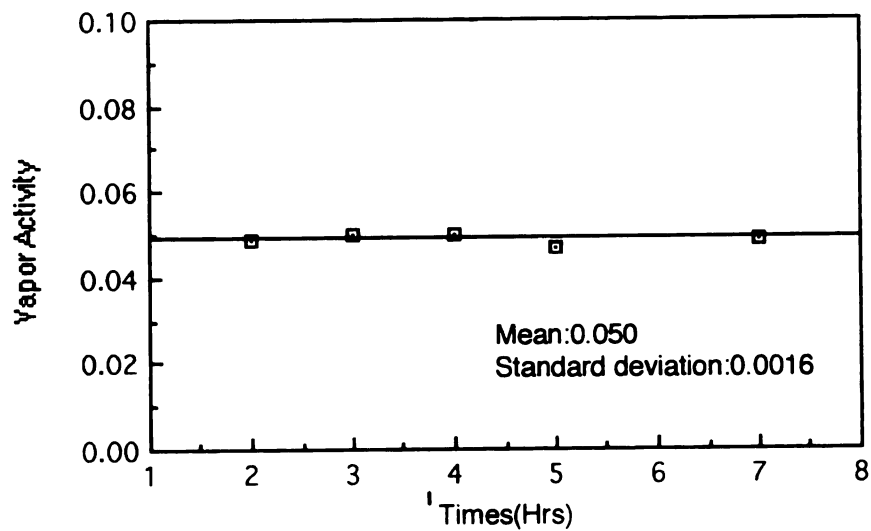


Figure 30. Distribution of vapor activity at $a = 0.050$

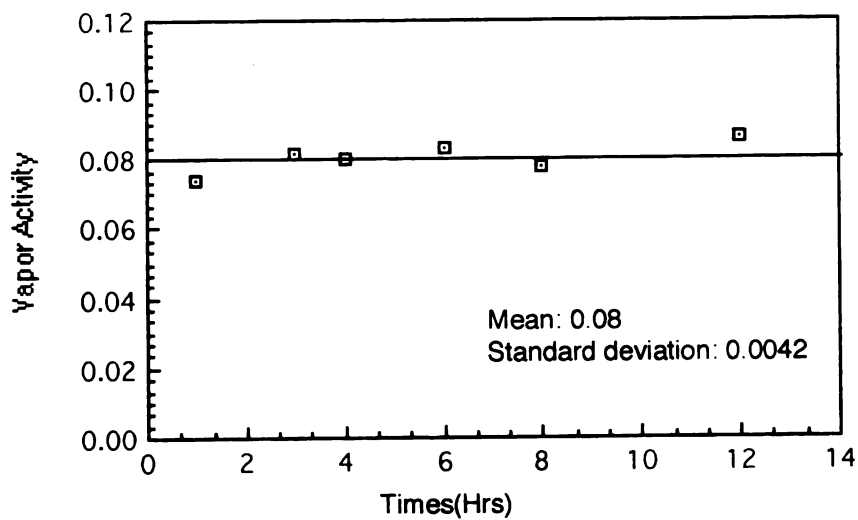


Figure 31. Distribution of vapor activity at $a = 0.080$

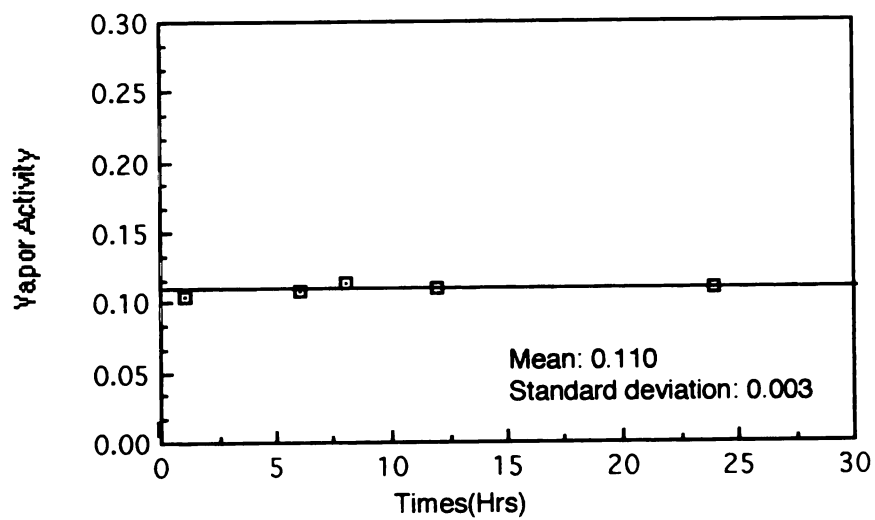


Figure 32. Distribution of vapor activity at $a = 0.110$

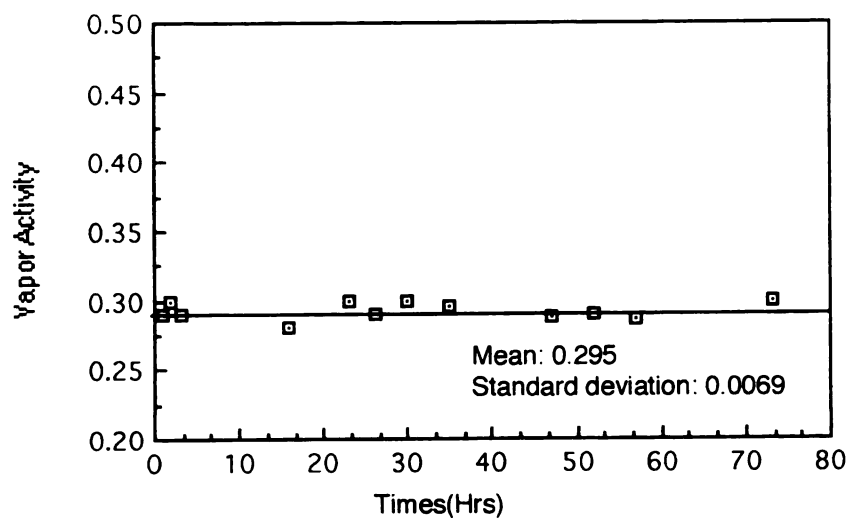


Figure 33. Distribution of vapor activity at $a = 0.295$

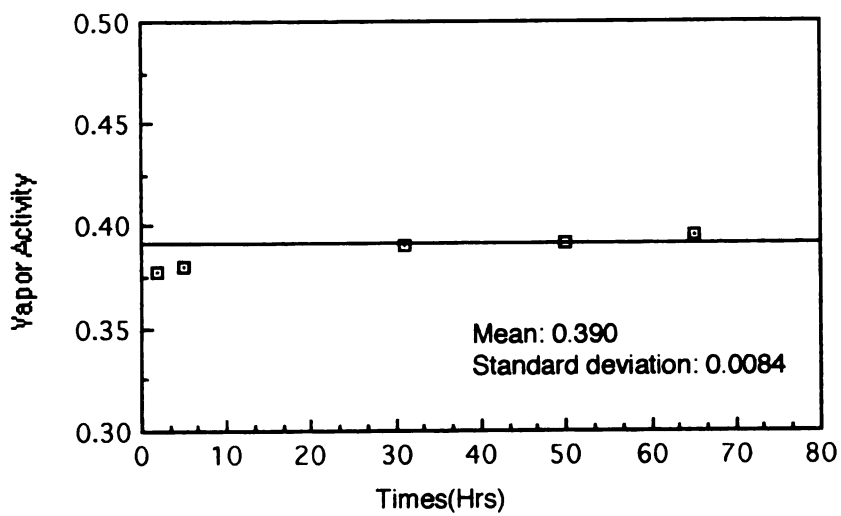


Figure 34. Distribution of vapor activity at $a = 0.390$

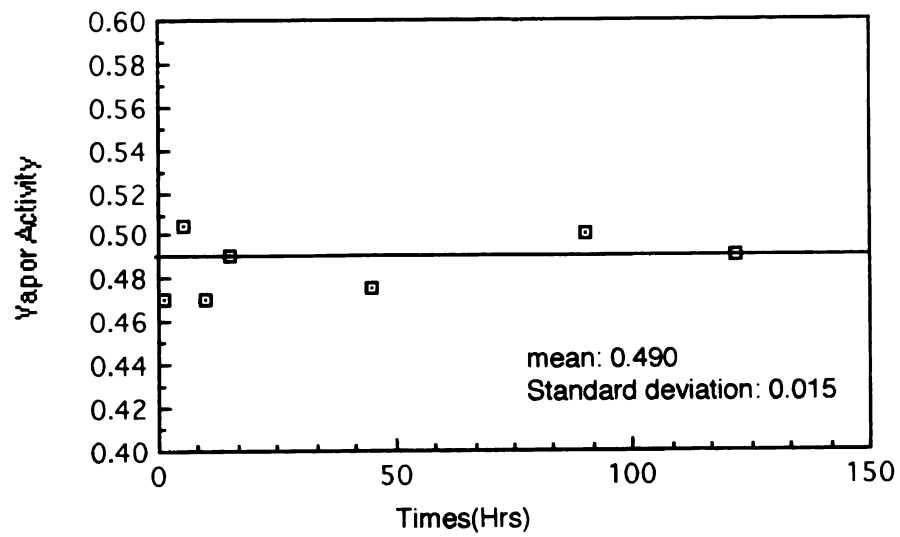


Figure 35. Distribution of vapor activity at $a = 0.490$

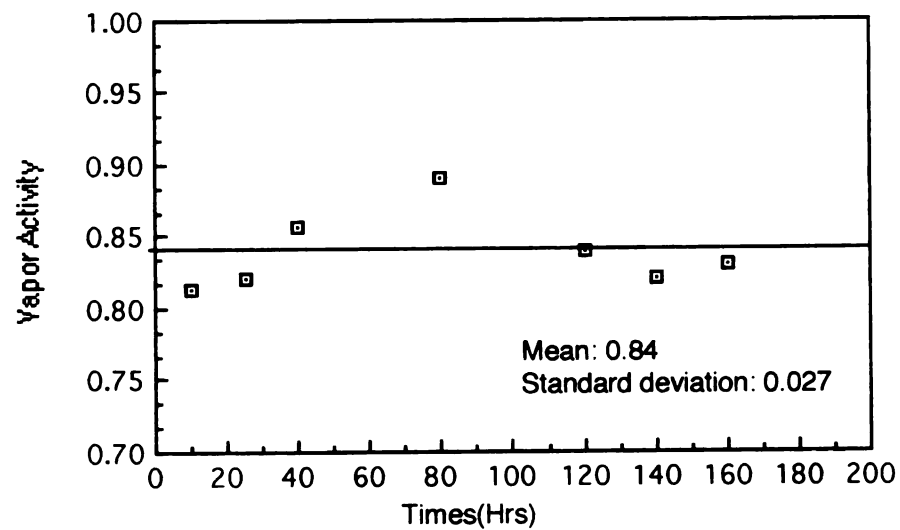


Figure 36. Distribution of vapor activity at $a = 0.840$

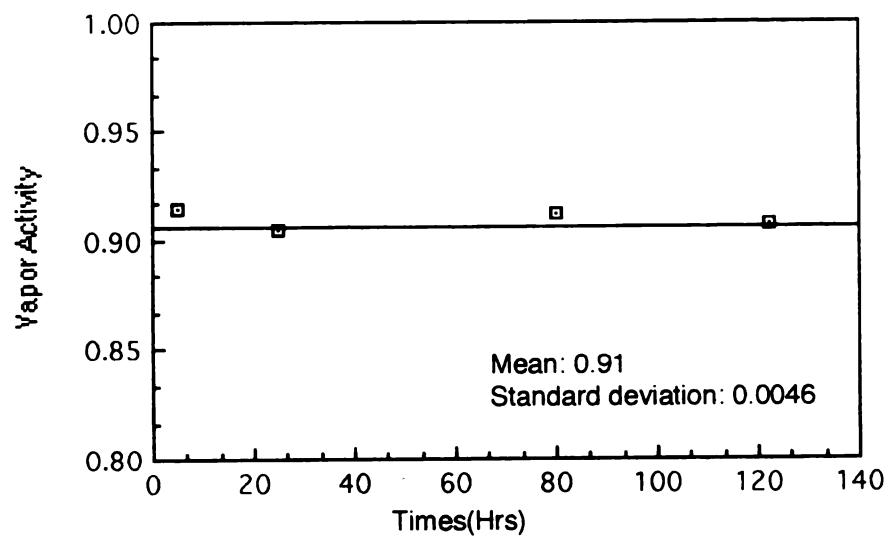


Figure 37. Distribution of vapor activity at $a = 0.910$

BIBLIOGRAPHY

- Bagley , F and F. A. Long., 1955. J. Am. Chem. Soc., 77 , 2172.
- Barrer, R., J.Barrie and J. Slater, 1957. J. Polymer Sci.,23, 315
- Beck, J . V and Arnold. K. J , 1977. "Parameter estimation in engineering science" , John Wiley and Son , New York , NY.
- Berens, A. R. 1975. Angew. Macromol. Chem., 47, 97.
- Blatz, P. S. 1989. "Innovations in polyamide technology" AICHE Meeting, Houston, TX, April 2 - 6.
- Blumstein, A., 1978. "Liquid Crystalline Order in Polymers", Academic Press, New York.
- Choy, C. L., W. P. Leung and T. L. Ma, 1984. J. Polym. Sci: Polym. Physics Edition, Vol. 22, 707-719
- Cohen, M. H. and D. Turnbull , 1959. J. Chem. Physics , 31 , 1164.
- Dolden, J G., 1976. "Structure property relationships in amorphous polyamides" Polym. Vol. 17 , pp 875
- Gedraitite, G. B., A. P. Martin and V. A. Shlyapnikov, 1989. Eur. Polym. J., 25:39.
- Gennes,P. G., 1979. "Scaling Concepts in Polymer Physics", Cornell Univ. Press, Ithaca, NY.
- Hartley, G. S. , 1946. Trans. Faraday Soc., 42B, 6.
- Hernandez, R. J., J. R. Giacin and A. L.Baner, 1986. J. Plastic Film and Sheeting, 2 (3) : 187.
- Hernandez, R. J., J. R. Giacin and E. A. Glulke, 1990. J. Membrane Science

Hopfenberg, H. B. and V. Stannett, 1973. "The physics of glassy polymers", R. N. Haward (ed), chapter 9, The diffusion and sorption of gases and vapors in glassy polymers, Applied science publishers Ltd, London, pp 504-506.

Kwei, T. K. and T. T. Wang, 1972. *Macromolecules*, 5, 128.

Meares, P., 1954. *J. Am. Chem. Soc.*, 76, 3415 - 22.

Meares, P., 1957. *Trans. Faraday Soc.*, 53, 101 - 6.

Meares, P., 1958. *Trans. Faraday Soc.*, 54, 40 - 6.

Michaels, A. S., W. Vieth and J. Barrie, 1963. *J. Appl. Phys.*, 34(1), 1, 13

Michaels, A. S. and H. J. Bixler, 1961. *J. Polym. Sci.*, 50, 393

Ohashi, K., R. J. Hernandez, J. R. Giacini and E. A. Gruke, 1991.
" Modeling the sorption of water vapor by a semicrystalline polyamide ",
Thesis, school of packaging, Michigan state univ.

Pace, R. J. and A. Datyner, 1980. "Model of sorption of simple molecules in polymer", *J. Polymer Sci.*, Vol. 18, 1103-1124

Pechhold, W. and H. P. Grossmann, 1979. *Disc. Faraday Soc.*, 68, 58.

Peterlin, A. 1975. *J. macromol. sci. physics*, B 11, 57

Rogers, C. E., 1965. " physics and Chemistry of the Organic solid state",
(Eds Fox, Labes, and Weissberger), Interscience, New York, Ch 6

Salame, M., 1986. *J. Plastic Film and Sheeting*, 2 (4): 321

Vieth, W. R., H. H. Alcalay and A. J. Frabe, 1961. *J. Appl. Polymer Sci.* 8, 2125.

Wendorff, J. H., 1987. "Studies on the nature of order in the amorphous polymers", International Symposium.

Williams, C., F. Brochard and H. L. Frisch, 1981. *Ann. Rev. Phys. Chem.* 32, 433-451.

MICHIGAN STATE UNIV. LIBRARIES



31293010250920